University of Southern Queensland

Faculty of Engineering & Surveying

Heat Transfer Measurements of a Re-entry Capsule Using Fast Response Thermocouples

A dissertation submitted by

Brody Roache

in fulfilment of the requirements of

ENG4112 Research Project

towards the degree of

Bachelor of Engineering (Mechanical)

Submitted: October, 2004

Abstract

Predicting the heat transfer of a re-entry capsule as it enters the atmosphere is critical to the capsule design. At hypersonic speeds, air temperature in front of a capsule entering the Mars atmosphere is heated to about 1600C by friction between the capsule and the gas in the atmosphere. An accurate heat transfer prediction is essential to design the heat shield as light as possible so that the scientific payload can be increased.

This project aims to investigate the application of fast response thermocouples to the measurement of heat transfer in the hypersonic flow produced by the gun tunnel, and obtaining representative data on selected re-entry capsule geometries for comparison with theory and other experiments.

E-Type thermocouples are used to calculate temperature change by measuring the emf produced by the Seebeck effect. Heat transfer is calculated by assuming one-dimensional heat conduction.

This project demonstrates that E-type thermocouples can be designed and constructed to effectively measure temperature with a response fast enough to effectively calculate heat flux during a 20 millisecond gun tunnel run.

University of Southern Queensland

Faculty of Engineering and Surveying

ENG4111/2 *Research Project*

Limitations of Use

The Council of the University of Southern Queensland, its Faculty of Engineering and Surveying, and the staff of the University of Southern Queensland, do not accept any responsibility for the truth, accuracy or completeness of material contained within or associated with this dissertation.

Persons using all or any part of this material do so at their own risk, and not at the risk of the Council of the University of Southern Queensland, its Faculty of Engineering and Surveying or the staff of the University of Southern Queensland.

This dissertation reports an educational exercise and has no purpose or validity beyond this exercise. The sole purpose of the course pair entitled "Research Project" is to contribute to the overall education within the student's chosen degree program. This document, the associated hardware, software, drawings, and other material set out in the associated appendices should not be used for any other purpose: if they are so used, it is entirely at the risk of the user.

Prof G Baker

Dean

Faculty of Engineering and Surveying

Certification of Dissertation

I certify that the ideas, designs and experimental work, results, analyses and conclusions set out in this dissertation are entirely my own effort, except where otherwise indicated and acknowledged.
I further certify that the work is original and has not been previously submitted for assessment in any other course or institution, except where specifically stated.

Brody Roache

0011122245

_____

Signature

_____

Date

Acknowledgments

I would like to thank my principal supervisor, Dr David Buttworth for his enthusiasm, support and cheerful advice, even after he had left the country. My assistant supervisor, Dr Ahmed Sharifian, who had been thrown in the deep end as my supervisor only six weeks before the due date. Also, the USQ Workshop staff for machining the thermocouples and the model - I know how much they dislike machining those small parts. I would like to thank my fellow classmates, from whom I sought much needed advice and support.

Finally, I would like to thank my parents, brothers, sister, and my girlfriend, Ammie, for their constant support and encouragement.

Brody Roache

University of Southern Queensland
October 2004

Contents

List of Figures

List of Tables

Nomenclature

c_p	Specific heat at constant pressure
c_v	Specific heat at constant volume
c_0	Speed of sound
D	Diameter
k	Thermal conductivity
Le	Lewis number
M	Mach number
MW	Molecular weight
N	Number of moles
n	Refractive index
Nu	Nusselt Number
P	Pressure
Pr	Prandtl number
Q	Quantity of heat
q	Rate of heat flow
q_c	Convection heat flow
q_k	Conduction heat flow
q''	Heat flux
R	Specific gas constant
R_u	Universal gas constant
Re	Reynolds number
S_{AB}	Seebeck coefficient for thermoelements A and B
St	Stanton number
T	Temperature

U	Flow velocity
V	Voltage
γ	Ratio of specific heats c_p/c_v
μ	Absolute viscosity
ρ	Density
ε	Dielectric constant
Subscripts	
∞	Free stream condition
01	Stagnation condition
02	Condition after normal shock
w	Wall condition

Chapter 1

Introduction

The development of hypersonic flow in high speed wind tunnels began in the late 1940's and the applications emerged in the 1950's. Since then, there has been continued research to improve the prediction of heat transfer of objects in hypersonic flow caused by heating due to friction between the gas and the object. For a re-entry vehicle, improving the heat transfer prediction allows better design of the heatshield. This is especially important for Mars missions as the payload is generally limited. An accurate heat transfer prediction allows the mass of the heatshield to be minimised so that the payload can be increased. This project investigates a simple, practical method of predicting heat transfer.

The aim of the project was to investigate the effectiveness of fast response type-E thermocouples in the measurement of heat transfer of a body in hypersonic flow. The thermocouples produce a data set temperature change history. Heat transfer is calculated by assuming one-dimensional heat conduction, taking the temperature history data as step inputs. If the study proves the type-E thermocouples to be effective, it provides a cheap and simple method of predicting heat transfer.

A background study was conducted in the areas of temperature measurement, heat transfer, Re-entry capsules, high velocity wind tunnels, hypersonic flow and hypersonic heat transfer. Chapters 2 and 3 are a review of the literature study.

An experiment was designed to conduct heat transfer measurements using type-E fast response thermocouples. The thermocouples were inserted into a small scale re-entry model and the model was tested in a gun tunnel to create a hypersonic flow. The gun tunnel is a high velocity wind tunnel and is designed to create a Mach 7 flow for 20 ms. The results were compared with a theoretical prediction using a modified version of the Fay and Riddell correlation.

Chapter 2

Hypersonic Heat Transfer

2.1 Chapter Overview

This chapter introduces the theory applied in later chapters as well as providing background information into the theory. The aim of this chapter is to broaden the scope of the theory, while the later chapters focus on the details. The topic of thermocouple temperature measurement is introduced by defining temperature and reviewing a selection of the many other systems of temperature measurement. Convection heat transfer, hypersonic flow and entry capsules are also discussed and provide background information for the final topic, hypersonic heat transfer.

2.2 Temperature

Temperature is a basic physical quantity that is used extensively in our daily lives, yet it is a quantity that is difficult to understand and measure. Temperature is an intensive quantity resulting in an inability to multiply or subdivide its units in order to measure over a wide range. Not only is temperature intensive but it has no close association with any easily perceived extensive quantity. A formal definition of temperature from Bedford (1990) is: *temperature is a thermodynamic quantity that takes the same value in two systems that are brought together into thermal contact and are allowed to reach*

thermal equilibrium. Thus temperature is the potential that governs the flow of heat.

2.3 Temperature Measurement

The measurement of temperature is a concept that is relatively recent, compared with other physical properties such as mass and length. The invention of the thermometer is credited to Galileo in 1592. His instrument was based upon the thermal expansion of air. Thermometers based on liquid-expansion followed soon after.

Temperature is a quantity that most physical properties are dependant on yet cannot be measured directly, unlike other quantities such as length and mass. In order to measure temperature, a system must be devised to calculate temperature based on a change in a physical property.

There are few physical properties that are not temperature dependant, hence there are many types of thermometers based on different physical properties. Thermal sensors may be divided into primary or thermodynamic sensors and secondary or practical sensors. Primary sensors have a relationship between the physical quantity and temperature that can be derived from first principles. Secondary sensors have an empirical relationship that requires a correlation developed from experiment. This section provides a brief introduction to the different types of sensors that have been developed.

2.3.1 Primary Thermal Sensors

A ***Gas Thermometer*** is based on the ideal gas law,

$$PV = NR_uT \tag{2.1}$$

where P is the absolute pressure, V is the volume, T is the absolute temperature, N is the number of moles and R_u is the universal gas constant. In a system with fixed mass, the number of moles is constant and temperature can be calculated from the measurement of pressure and volume, It is true for a real gas at low pressures and densities, and its application and measurement is simple.

An ***Acoustic Thermometer*** also assumes an ideal gas and is based on the change in speed of sound which is defined as,

$$c_0^2 = \frac{\gamma RT}{MW} \tag{2.2}$$

Measurement of the speed of sound is achieved by using a transducer to set up a resonant standing wave at a known frequency inside a cylindrical gas column. The wavelength can be measured to calculate the speed of sound, and hence, temperature.

A ***Dielectric Constant Thermometer*** is based on the Clausius-Mossotti equation,

$$\frac{(\varepsilon - 1)}{(\varepsilon + 2)} = \frac{A_\varepsilon N}{V} \tag{2.3}$$

which relates the dielectric constant, ε, of an ideal gas to the molar polarisability, A_ε. Temperature can be calculated by substituting V from equation 2.1,

$$P = \frac{(\varepsilon - 1)R}{(\varepsilon + 2)A_\varepsilon} T \tag{2.4}$$

For a real gas a virial expansion for the dielectric constant is required to increase the accuracy.

Temperature can be calculated using the refractive index of a medium in the same way the dielectric constant is used. The dielectric constant of a gas is related to its refractive index by $n^2 = \varepsilon$ so that,

$$P = \frac{(n^2 - 1)R}{(n^2 + 2)A_\varepsilon} T \tag{2.5}$$

Expressing in terms of the refractive index presents opportunities for different methods for taking measurements.

A ***Total Radiation Thermometer*** is based upon the the measurement of thermal radiation, either total or spectral, and therefore no physical contact with the medium is required. The principle of this thermometer is derived from Plank's Law

$$L_\lambda(T)d\lambda = c_1 \lambda^{-5} n^2 (e^{c_2/\lambda T} - 1)^{-1} d\lambda \tag{2.6}$$

which relates the spectral radiance, $L_\lambda(T)$, of a blackbody to wavelength, λ, and temperature, T, where c_1 and c_2 are the first and second radiation constants.

When integrated over all wavelengths, the total radiant exitance, $M(T)$ in W/m^2, is expressed simply as $M(T) = \sigma T^4$ for a blackbody or

$$M(T) = \varepsilon \sigma T^4 \tag{2.7}$$

for a real surface where ε is the total emissivity in the direction of view and σ, Boltzmann constant equals $5.67 \times 10^{-8}\, W/(m^2 K^4)$.

Other primary sensors include *Noise, He Melting Curve, Nuclear Orientation, Vapour Pressure, Magnetic and Spectroscopic Thermometers.*

2.3.2 Secondary Thermal Sensors

Electrical Resistance thermometry is a simple, reliable and sensitive method of temperature measurement. It is based on the variation of resistance with temperature, which is measured from the voltage drop across the resistor when a fixed current is applied.

Thermal Expansion thermometers were the basis of the early thermometers 400 years ago and are still the most common of all thermal sensors. There are three main types of thermal expansion sensors:

Liquid in Glass. A liquid in glass sensor relies on the difference in thermal expansion between the liquid and glass bulb to force the liquid along a capillary tube in the glass as the temperature changes. A graduated scale is provided along the tube and the reading is taken from the top of the liquid column.

Filled System. While this method assumes thermal expansion theory, temperature is measured from variation in pressure. The expansion of the liquid in a confined volume exerts a pressure. The pressure can then be measured by numerous means.

Bimetallic. sensors make use of the difference in thermal expansion among different metals. If two different metals are bonded together to form a cantilever, a change in temperature creates a deflection. If the metals are bonded to form a helix with one end fixed, a more pronounced angular deflection is produced and the free end can be attached to a needle so that temperature can be read off a calibrated dial.

Thermoelectric sensors rely on the conversion of thermal energy to electrical energy. This phenomenon is known as the Seebeck effect. An electric current will flow in a closed circuit of two or more different conductors when there is a temperature change between the junctions. Thermoelectric sensors or thermocouples are discussed in detail in the following section.

2.4 Thermocouples

A thermocouple is a thermoelectric thermal sensor and is one of the most common temperature measurement instrument for industrial and commercial applications as they are inexpensive, simple and robust. Thermocouple materials are internationally standardised, making the materials cheap and easily available as well as increasing accuracy and simplifying calibration. Appropriate choice of thermoelements can provide accuracy over a wide range of temperature as well as being able to withstand many types of corrosive atmospheres.

In 1821, Johann Seebeck discovered that if two conducting wires of different metals were connected by their ends to create a complete electronic circuit, illustrated in figure 2.1, then a small current will flow if the junctions are at different temperatures. The electrical potential created by the temperature difference is known as the Seebeck electromotive force (emf). The magnitude of the emf is proportional to the change in temperature:

$$dV_{AB} = S_{AB}dT \tag{2.8}$$

where S_{AB} is the Seebeck Coefficient. The Seebeck Coefficient depends on the two materials used.

The properties of themocouples can be summarised by the three basic laws of thermocouples:

1. *A thermal emf is not generated in a circuit of a homogeneous conductor regardless of temperature change.*

   Therefore at least two different materials are required for a thermoelectric circuit.

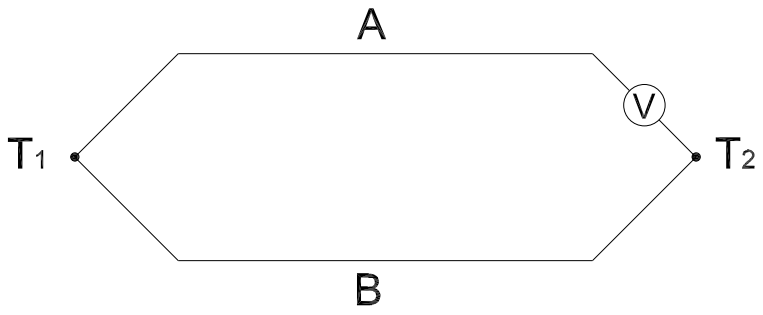

Figure 2.1: Thermocouple circuit.

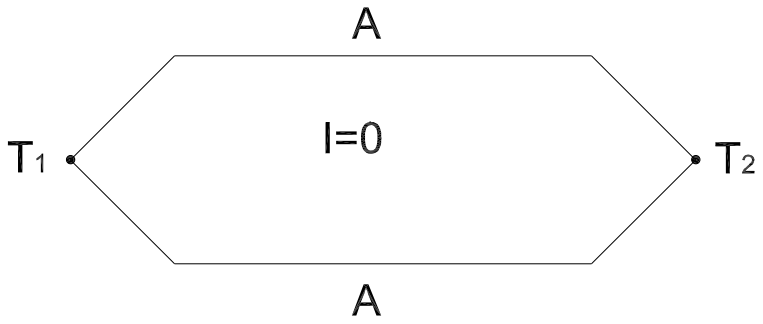

Figure 2.2: First law of thermocouples.

An emf generated in a circuit that is supposed to be homogeneous shows that there are impurities present. Also, when a thermocouple is made up of two or more homogeneous conductors, the temperature variation along homogeneous sections has no effect on the emf. The law is illustrated in figure 2.2.

2. *A thermal emf is not generated in a circuit of any number of different conductors if the junctions are held at constant temperature.*

   No matter what dissimilar conductors are in contact with the thermoelectric circuit, there is no effect if the junctions are at the same temperature (figure 2.3).

3. *The thermal emfs generated in a circuit are additive*

   The emf from a lower temperature to a higher temperature is equal to the sum the emf from the lower temperature to an intermediate temperature and the emf from that intermediate temperature to the higher temperature and is described mathematically as:

$$\int_{T_1}^{T_3} S_{AB} dT = \int_{T_1}^{T_2} S_{AB} dT + \int_{T_2}^{T_3} S_{AB} dT \tag{2.9}$$

   and illustrated in figure 2.4.

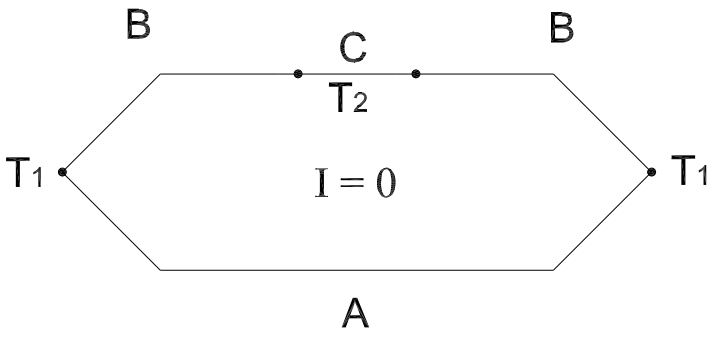

Figure 2.3: Second law of thermocouples.

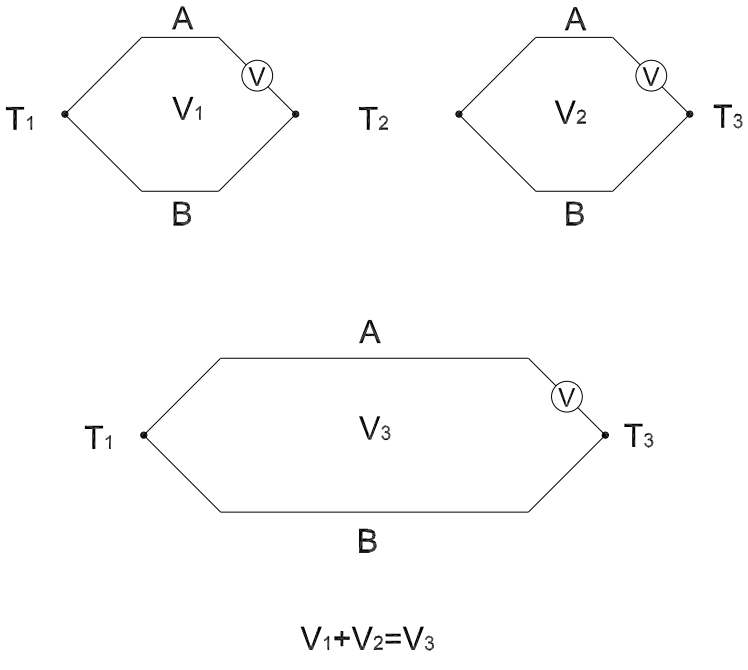

Figure 2.4: Third law of thermocouples.

Design of the thermocouples used in this project are discussed in Chapter 4, E-Type Fast Response Thermocouple.

2.5 Convection Heat Transfer

Whenever a temperature gradient exists within a system, or when two systems at different temperatures are brought into contact, heat energy is transferred. There are three distinct modes of heat transfer: conduction, radiation and convection. Convection is theoretically only a quasi mode of heat transfer, as it is a form a of conduction.

The convection mode of heat transfer comprises of two mechanisms acting simultaneously. The first is heat conduction which is described as motion among individual molecules. The second is the macroscopic motion of fluid particles consisting of large numbers of molecules that are subjected to a force. The force can be in the form of an external force such as a fan, and is called forced convection. Natural convection occurs when a force is created by a change in pressure resulting from the temperature change in the fluid. Convection heat transfer is directly proportional to the difference in temperature between the surface and the free stream fluid temperature.

As a fluid in motion approaches a surface the velocity decreases as a result of viscous forces. The section of flow that is affected by the surface is called the boundary layer. Since the velocity at the surface is zero, the heat transfer between the surface and the fluid layer ($y = 0$) must be by conduction:

$$q''_k = -k_f \frac{\partial T}{\partial y} \tag{2.10}$$

where k_f is the thermal conductivity of the fluid. The Temperature gradient at the surface $\frac{\partial T}{\partial y}$ is determined by the rate at which the flow dissipates the heat energy away from the surface. The general equation for convection heat transfer is:

$$q_c = \bar{h}_c A(T_s - T_\infty) \tag{2.11}$$

where $\bar{h}_c$ is the average convection heat transfer coefficient. In laminar flow the heat transfer coefficient can be calculated using exact mathematical solutions of the boundary layer equation, providing there is sufficient information for the fluid properties. If

the velocity is high and the the flow is turbulent then empirical methods must be used to approximate the heat transfer coefficient.

2.6 Hypersonic Flow

Hypersonic flow is generally accepted as flow where the Mach number, M, is greater than 5. The mach number is a dimensionless number that describes the speed of an object in terms of the local speed of sound, given by:

$$M = \frac{U}{c_0} \tag{2.12}$$

where the speed of sound, c_0, is given by:

$$c_0 = \sqrt{\gamma RT} \tag{2.13}$$

Subsonic flow is flow speed that is less than the speed of sound ($M < 1$). Transonic flow is the term for flow between $M = 0.8$ and $M = 1.2$. Supersonic flow is the flow regime above Mach 1.2. At supersonic flow, characteristics of the flow are different from subsonic flow and certain flow phenomena become evident.

The most distinguished of these is the presence of a shock layer. A shock layer is a high pressure wave in front of an object in supersonic flow. The wave is created by the sudden change in velocity in the flow due to the presence of the object. Figure 2.5 is a photograph of the entry capsule model during the gun tunnel run. The shock wave can be seen in front of the model (photograph courtesy of David Sercombe).

Hypersonic flow is a regime beyond supersonic flow, usually $M > 5$, where certain supersonic flow conditions become increasingly evident. Anderson (1989) defines hypersonic flow as the regime where the following physical phenomena occur:

Thin Shock Layers Oblique shock theory states that for a given flow deflection angle, the density increase across the shock wave increases as the Mach number is increased. At higher density, less space is required for the fluid to pass around the body and hence the shock layer becomes increasingly smaller.

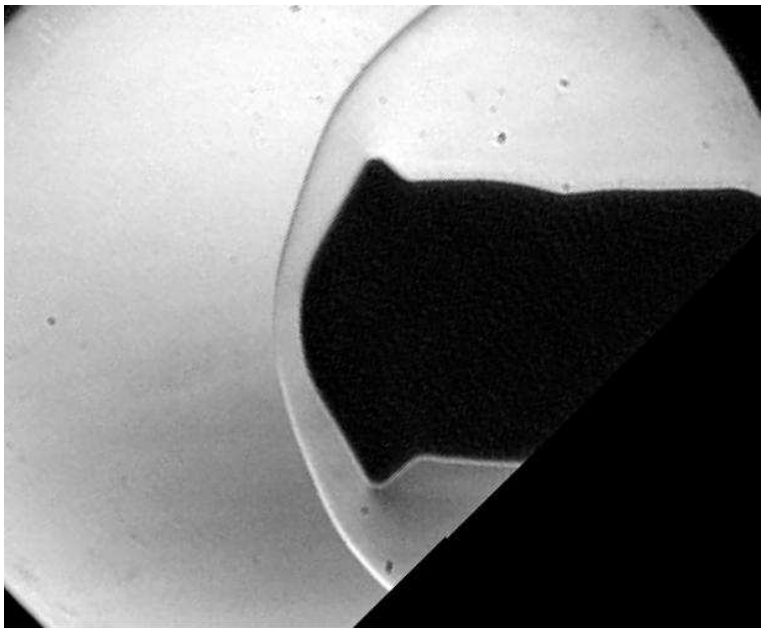

Figure 2.5: Shock wave produced by the model in hypersonic flow.

Entropy Layer The entropy of the flow increases across a shock wave, and the stronger the shock the greater the entropy increase. Because the nose region is highly curved there are strong entropy gradients generated at the nose. This entropy layer flows downstream along the surface.

Viscous Interaction High velocity, hypersonic flow contains a large amount of kinetic energy. When the flow is slowed by the viscous effects within the boundary layer, part of the kinetic energy is transformed into internal energy of the gas, which increases the temperature of the gas. The characteristics of the boundary layer are dominated by temperature profile. The viscosity coefficient increases with temperature, forcing the boundary layer to become thicker, and the density increases, further enlarging the boundary layer. The thick boundary layer affects the inviscid flow outside the boundary layer. The change in inviscid flow in-turn affects the boundary layer. This interaction between the viscous and inviscid flow is called viscous interaction.

High-Temperature Flows As hypersonic flow is slowed by the viscous effects, the transformation of kinetic energy to internal energy can be enough to cause dissociation and ionisation of the gas.

Low Density Flow At the upper regions of the atmosphere where hypersonic flow is

applicable, the air no longer acts as a continuous medium. The average distance, λ, that individual molecules travel between collisions equals about 30 cm. Under these conditions conventional aerodynamic concepts based on the assumption of continuum begin to break down. Specifically, the assumption that flow velocity slows to zero due to friction. At low densities the velocity takes a finite value. This is called the velocity slip condition. While low density flow is not an effect of hypersonic flow, it is important, as most hypersonic vehicles, in particular re-entry vehicles, experience such phenomena.

2.7 Entry Capsule

An entry, or re-entry capsule is a vehicle designed for entering the atmosphere from space. The most famous of these are the Apollo "Command" capsule and the space shuttle. Other notable entry vehicles include the Gemini, Mercury, and the Mars landers, Viking I and II. More recent Mars entry capsules include the Pathfinder, Mars Exploration Rovers (MER) and Beagle 2. The Pathfinder and MER were both NASA programs and were based on the Viking design. The Beagle 2 lander was part of the Mars Express program by the European Space Agency.

Tremendous heating occurs during re-entry into the atmosphere, and therefore, prediction of the heat transfer is vital to the design of the entry vehicle. To maximise the available payload, the minimum mass of heat shield is desired, hence the need for more accurate predictions of heat transfer.

The Beagle 2 was a low budget, yet highly ambitious, project to send a lander to Mars, onboard the Mars Express. The total mass of the Beagle 2 was 60 kg, yet it was fitted with more scientific instruments than any other Mars mission to date. Unfortunately, communication was lost with the Beagle 2 shortly after it jettisoned from the Mars Express.

Two scale models of the Beagle 2 were produced for the heat transfer measurement experiment. The Beagle 2 capsule, or entry system, consists of an aeroshell (front cover), bioshield (back cover) and release mechanisms. The aeroshell is a 60° half-angle

cone with a maximum vehicle diameter, D, of 0.9 m. It has a blunted nose and a curved shoulder with specific radii designed to evenly distribute the heat load.

2.8 Hypersonic Convection Heat Transfer

At hypersonic conditions, the temperature of the gas is heated to extremely high temperatures in the shock layer. Heat energy from the high temperature gas is convected and radiated into the object. An enormous amount of heat energy is generated when an object travels at hypersonic velocities. For example, when the Apollo capsule entered the atmosphere it slowed down from 11 km/s to a subsonic velocity. Therefore 3.57×10^5 MJ of kinetic energy was converted into heat energy. Determining the amount of heat transferred into the object cannot be calculated purely from theory.

There are numerous correlations to calculate convection heat transfer in a hypersonic flowfield. One of the most general equations for stagnation heat transfer is by Fay and Riddell (1958) as published by Bertin (1994). The correlation is:

$$q'' = \frac{0.763}{Pr^{0.6}}(\rho_{02}\mu_{02})^{0.4}(\rho_w\mu_w)(H_0 - h_w)\left[1 + (Le^{0.52} - 1)\frac{h_d}{H_0}\right]\left[\left(\frac{du_e}{dx}\right)_0\right]^{0.5} \tag{2.14}$$

where,

$$Le = \frac{\rho D_{12} c_p}{k}$$

Le is the Lewis-Seminov number, D_{12} is the binary diffusion coefficient for a mixture of two gases, Pr is the Prandtl number, H_0 is the total stagnation enthalpy, h_w is the enthalpy at the wall and h_d is the average atom disassociation energy multiplied by the atom mass fraction at the edge of the boundary layer. This equation is often simplified by approximating the Lewis-Seminov number to zero.

One of the pioneer correlations for hypersonic heat transfer is by Detra et al (1957), as cited in Anderson (1989), who developed this correlation for flight applications:

$$q'' = \frac{11030}{R_N^{0.5}}\left(\frac{\rho_\infty}{\rho_{SL}}\right)^{0.5}\left(\frac{U_\infty}{U_{CO}}\right)^{3.15} \tag{2.15}$$

where R_N is the nose radius, U_{CO} is the circular orbit velocity and ρ_{SL} is density at standard sea level conditions.

White (1991), as cited by Buttsworth & Jones (2003), developed a similar correlation to that of Fay and Riddell (1958). It defines the stagnation point heat transfer coefficient for a sphere at any Mach number:

$$Nu = 0.736 Pr^{0.4} Re^{0.5} C^{0.1} \left(\frac{KD}{U_\infty}\right)^{0.5} \tag{2.16}$$

where

$$\begin{aligned} Nu &= \frac{h_c D}{k} \\ Pr &= \frac{c_p \mu_{02}}{k_{02}} \\ Re &= \frac{\rho_{02} U_\infty D}{\mu_{02}} \\ K &= \frac{du_{02}}{dx} \\ C &= \frac{\rho_w \mu_w}{\rho_{02} \mu_{02}} \end{aligned}$$

Meese & Nørstrud (2002) developed the following correlation for heat flux for re-entry at stagnation:

$$q_c'' = K_s \rho_0^{0.5} V_{entry}^3 \frac{\exp\left(\frac{-\beta z}{2}\right)}{[1 + b\exp(-cz)]^{3/2}} \tag{2.17}$$

where K_s is the scaling factor for convective heat flux model at stagnation, β is the scaling parameter for atmospheric density, m^{-1}, z is altitude in metres, b is the model parameter for logistic re-entry curve and c is model parameter for re-entry curve.

2.9 Chapter Summary

In summary, it was found that temperature is an intensive physical property, making it impossible to measure directly. However, most physical properties are temperature dependant and hence there are numerous methods for measuring temperature indirectly.

A thermocouple is a thermoelectric thermometer. Change in temperature is calculated by measuring the emf that is produced by the Seebeck effect.

In general heat transfer is a function of the temperature change. Convection heat transfer also depends on the properties of the flow. Convection heat transfer in hypersonic and supersonic flow is much harder to predict than subsonic flow because of certain physical phenomena that occur above the speed of sound. However there have been many correlations devised to predict heat transfer under such conditions. Knowledge in this area has been vital in the success of space flight and military missiles.

Chapter 3

USQ Gun Tunnel

3.1 Chapter Overview

The USQ gun tunnel provided the testing conditions for the experiment and therefore, reviewing the operation of the gun tunnel and the theory behind it was an important stage in this project. This chapter investigates the theory and performance of the USQ gun tunnel and discusses its advantages and limitations. Brief introductions into other types of high speed wind tunnels are provided as a background into the topic and also to compare and contrast with the gun tunnel.

3.2 Wind Tunnels

A wind tunnel is designed to create a flow-field under controlled conditions. The earliest wind tunnels coincided with the invention of manned flight. The first known wind tunnel was designed by the Wright Brothers in 1901. The development of near transonic wind tunnels began in the 1930's and by the end of world war two numerous supersonic wind tunnels existed. However it was in the decade post-world war two that the development of supersonic and hypersonic wind tunnels flourished. The phenomenon at the throat and the creation of a shock wave were two important discoveries during the development of supersonic wind tunnels. In subsonic flow, velocity is increased by

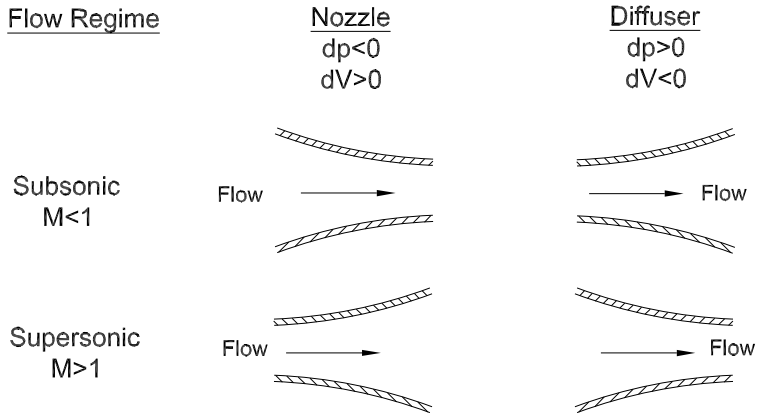

Figure 3.1: Difference between subsonic and supersonic flow (Fox & McDonald 2004).

using a converging nozzle whereas in supersonic flow, a converging nozzle slows the velocity to Mach 1. To increase the velocity of a supersonic flow, a diverging nozzle must be used, as illustrated in figure 3.1. A diverging nozzle expands and accelerates the air. The stored energy in the flow is converted into kinetic energy. Therefore, a large amount of energy must be added to the gas before entering the nozzle. The main difference between the various types of high speed wind tunnels is the method of adding the energy to the flow. Power is proportional to velocity cubed, therefore hypersonic wind tunnels consume a tremendous amount of power compared to subsonic wind tunnels.

There are numerous types of high velocity wind tunnels, each with their own advantages, disadvantages and specific applications. The following is a summary of the most common high velocity wind tunnels, excluding gun tunnels. Gun tunnels are described in the following section.

Hotshot Tunnel An impulse wind tunnel that depends on the explosive release of energy to rapidly increase the temperature and pressure of the test gas held in the arc chamber. The small volume of test gas expands and accelerates through a nozzle into the test section to create a hypersonic flow for around 100 ms. The arc chamber is pressurised and the test section is evacuated to a very low pressure. The high and low pressures are separated by a thin diaphragm. An electric arc is used to generate the high temperature and pressure.

Plasma Arc Tunnel A tunnel that also uses an electric arc to generate high temperature gas. A plasma arc tunnel is different to a hot shot tunnel in that in can operate continuously. The disadvantage is that it operates at low densities and supersonic rather than hypersonic velocities. The plasma arc tunnel consists of an arc chamber, a nozzle, an evacuated test section and a vacuum system to maintain a low pressure in the test section. Test gas flows through the arc chamber where an electric arc raises the gas to ionisation level. The test gas becomes a mixture of free electrons, positively charged ions and neutral atoms. The temperature of the test gas is enough to vaporise the nozzle, so a water cooling system must be used. The capability of the nozzle to withstand high temperature defines the test time and is generally a couple of minutes. Plasma arc tunnels are most commonly used for testing heatshield materials.

Shock Tunnel Like a hotshot tunnel, a shock tunnel is an impulse tunnel but it differs in the way energy is added to the test gas. A shock tunnel has a driver section attached upstream of the test gas. The driver section is separated from the test gas by a diaphragm and is pressurised. When the diaphragm bursts, a shock wave is created that accelerates and compresses the test gas. When the shock wave reaches the end of the driven tube it is reflected and further heats the test gas. The test gas bursts through the second diaphragm into the nozzle. Shock tunnels provide high temperature and pressure conditions but have test times in the order of milliseconds.

Expansion Tube This tunnel begins the same as a shock tunnel with a high pressure driver gas separated from the test gas by a diaphragm. The resulting shock wave encounters a second low pressure diaphragm that ruptures on contact. The third chamber is at a very low pressure which cools and accelerates the test gas. The test is therefore high velocity and low temperature and pressure, similar to the upper atmosphere conditions applicable for a re-entry vehicle.

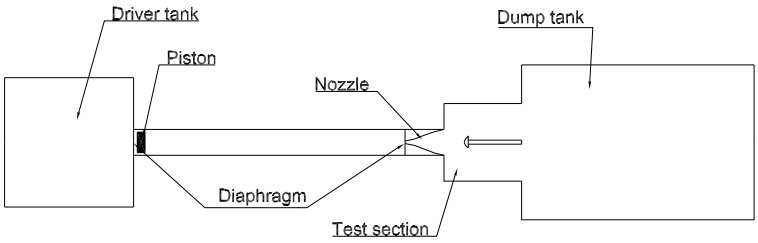

Figure 3.2: Schematic diagram of a gun tunnel.

3.3 Gun Tunnel

Like the shock tunnel, the gun tunnel includes a high pressure driver section a low pressure driven section and a diaphragm separating the two. A schematic diagram of a gun tunnel is shown in figure 3.2. A piston is placed adjacent to the diaphragm so that when the diaphragm bursts, the piston is propelled down the barrel. The piston accelerates to a supersonic velocity that compresses the driven gas and also creates a shock wave in front of the piston that heats the driven gas. The shock wave is reflected off the end of the tube and back to the piston, causing further heating of the gas. The heated and compressed test gas ruptures a second diaphragm and flows through the nozzle to the test section.

The test time for a gun tunnel is limited by the length of the barrel and is generally about 20 ms. An advantage that a gun tunnel has over a shock tunnel is that the test time is about an order of magnitude longer. However, a gun tunnel cannot achieve the high pressure and temperature created in a shock tunnel. The piston is the limiting factor in the design of a gun tunnel. It must be durable enough to withstand the high temperature and impact loading conditions but also light so that minimal energy is wasted by accelerating it.

3.4 USQ Gun Tunnel

The gun tunnel at the University of Southern Queensland is located in S Block, Toowoomba Campus. It produces a stagnation pressure of either about 2.7 MPa or 6 MPa depending on the diaphragm used and has a nozzle designed to create a Mach 7.0 flow. The following sections describe in further detail the operation of a gun tunnel, specific to the facility at USQ.

3.4.1 Driver Section and First Diaphragm

The driver tank is a cylindrical steel tank measuring about 3 m long and about 0.5 m in diameter. The tank can be filled with various gases but air is generally used. The aim of the driver section in any wind tunnel is to compress and heat the test gas before it flows through the nozzle. Heat is to prevent liquefaction of the test gas. Liquefaction occurs when the initial temperature of the gas allows the expansion of the gas in the nozzle to cool it to the liquid phase. The aim of the driver tank for the gun tunnel is to provide high pressure to force the piston down the barrel at high velocity and produce a high stagnation pressure and temperature in the test gas.

The driver tank is separated from the barrel by a diaphragm. The diaphragm is made from a 1 mm thick aluminium plate. A single plate can create a stagnation pressure of 3 MPa. Two plates can be used to double the stagnation pressure. The driver is compressed until either the diaphragm bursts or manual trigger is used. The manual trigger can be used to control the stagnation pressure. Figure 3.3 shows the position of the driver tank with respect to the rest of the gun tunnel.

3.4.2 Barrel and Nozzle

The barrel is connected to the driver tank at one end and the nozzle at the other end. A diaphragm is placed between each junction. The diaphragm at the driver tank is aluminium, as previously mentioned and the diaphragm at the nozzle is made from a piece of cellophane. The inside diameter of the barrel is 80 mm and is about five metres

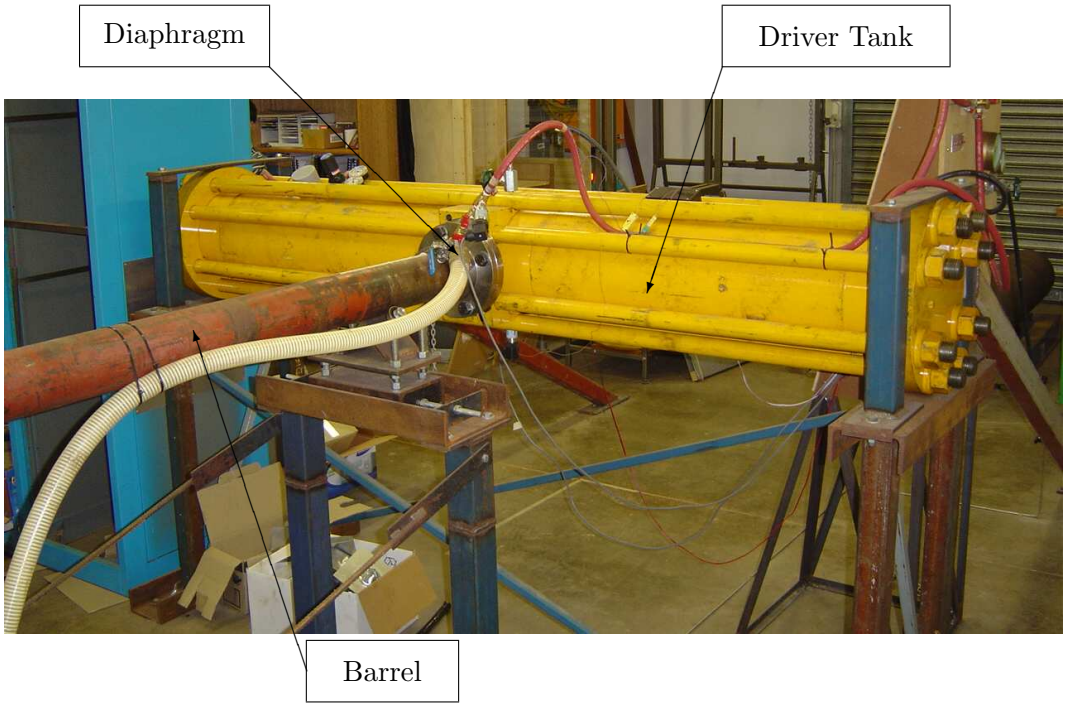

Figure 3.3: The driver tank.

long. Inside the barrel is a plastic piston. The piston is 50 mm long and is made from high strength, light-weight plastic. It is placed adjacent to the first diaphragm.

When the first diaphragm ruptures, the pressure difference between the driver and driven gas causes the driver gas to force the piston down the barrel. The force is due to the driver and driven gases attempting to reach an equilibrium position. The piston compresses the driven gas and the shock wave created by the supersonic flow heats the gas. At about the time the system reaches equilibrium, the second diaphragm bursts and the heated and compressed test gas flows through the nozzle to the test section. It takes about 50 ms for the test gas to be forced through the nozzle. The momentum of the piston forces it to overshoot the equilibrium position momentarily. This is the cause of the initial spike in the pressure history. Figure 3.4 is a plot of the stagnation pressure history measured by a pressure transducer at the end of the barrel during a gun tunnel run. The initial spike in the plot is caused by the overshoot of the piston. A schematic diagram of the different pressures in the gun tunnel at different stages of the run is shown in figure 3.5

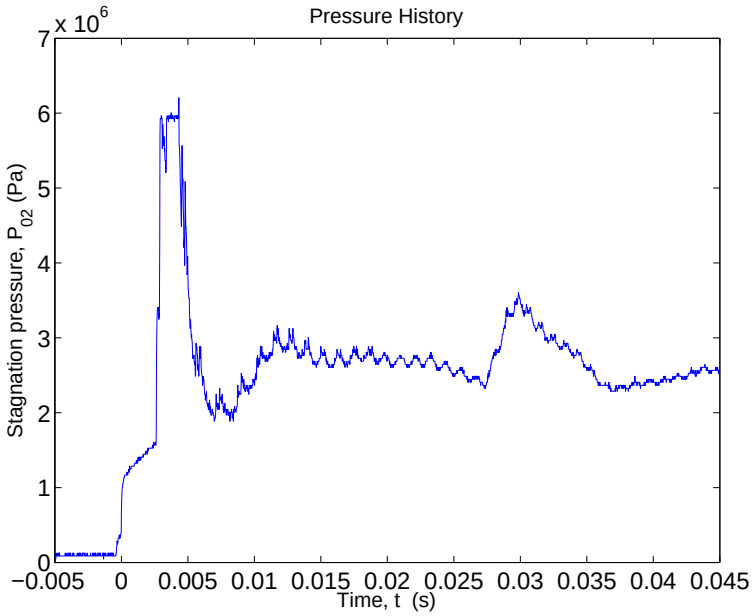

Figure 3.4: Pressure history from experiment.

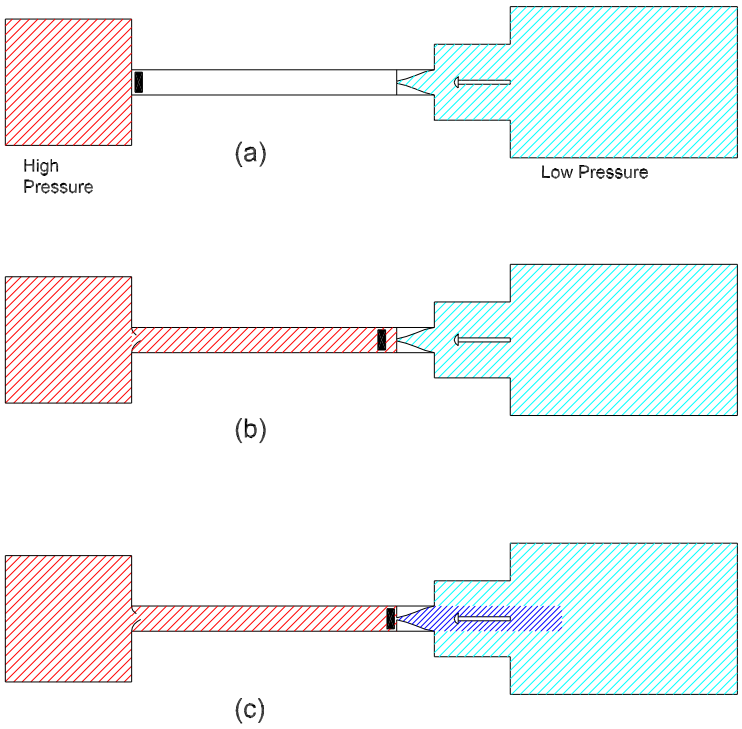

Figure 3.5: Pressure differences in the gun tunnel at (a) Before the first diaphragm ruptures; (b) Before the second diaphragm ruptures; and (c) during the test time.

The nozzle is designed to create a Mach 7 flow. The final diameter of the nozzle is 80 mm. In supersonic and hypersonic flow, the nozzle expands and accelerates the flow. At the throat, the point of the smallest diameter in the flow, the velocity of the flow becomes transonic. In the expansion section of the nozzle, the flow expands and accelerates as the stored energy in the gas is converted to kinetic energy. The shape of the nozzle relates to figure 3.1, for $M > 1$ and is designed to minimise losses and also to reduce the boundary layer thickness so that disturbances in the flow are minimised and the effective cross-sectional area is maximised.

3.4.3 Test Section and Dump Tank

The test section is connected to the end of the nozzle and the dump tank butts onto the end of the test section. While the driver tank is compressed, the test section and dump tank is partially evacuated to increase the pressure ratio. The dump tank is a large pressure vessel about twice the size of the driver tank. It allows a stable flow of the test gas, by providing a large volume for the test gas to flow into. The test section is a cube shape with windows on the sides. A sting is mounted into the front of the dump tank. A sting is a device designed by Terhorst (2001), a previous project student, to fix the test piece in the test section. It was designed to hold a scale model of a re-entry capsule and the associated measuring instruments. It has various mounting positions so that a variety of angles of attack could be analysed.

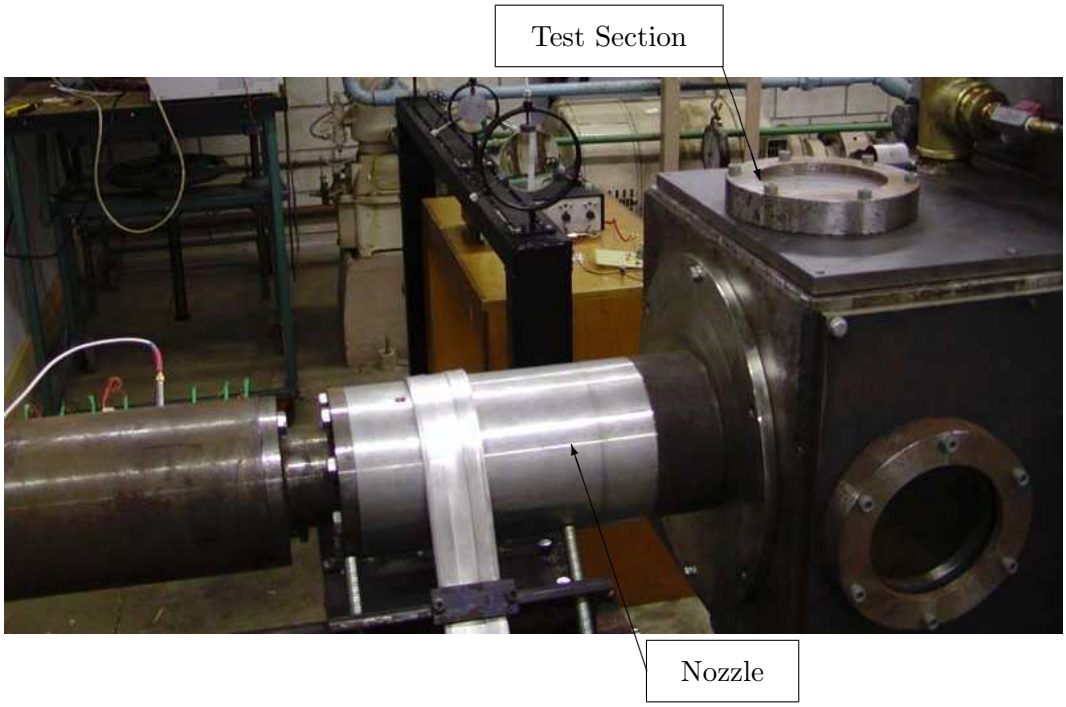

Figure 3.6: The test section of the gun tunnel.

3.5 Chapter Summary

Wind tunnels are research tools designed to simulate flow fields under controlled conditions. There are many types of hypersonic wind tunnels but the only major difference between them is the driver section. The driver section adds energy to the test gas, usually through heat and compression. An enormous amount of energy is required for hypersonic tunnels compared to subsonic tunnels. This is because power is proportional to velocity cubed and because the shock wave in supersonic flow consumes a large amount of energy.

A gun tunnel consists of a driver tank, barrel, nozzle, test section, and dump tank. A high pressure diaphragm is placed between the driver tank and barrel and a lower pressure diaphragm is placed between the barrel and nozzle.

The USQ gun tunnel is designed to produce a Mach 7 flow with a 20 ms effective test time. A stagnation pressure of either 3 MPa or 6 MPa is created, depending on whether one or two aluminium plates are used. The effective cross-sectional area of the flow is 80 mm.

Chapter 4

E-Type Fast Response Thermocouple

4.1 Chapter Overview

This chapter investigates the design, construction and calibration of the thermocouples used in the experiment. In the design section, the process of designing the thermocouples, and the final design is described. The construction and calibration sections describe the challenges and processes involved in the respective stages of the thermocouple development.

4.2 Design

The initial stage of the design process is to establish the design criteria. It states the objectives and restraints of the design. The objectives and restraints of the design must be determined so that the design process remains focused on the objectives and the limitations are clearly defined.

The objective was to design fast response thermocouples for surface temperature measurement of a small scale model in hypersonic flow. They must be accurate, inexpensive

and simple to construct. The main constraint in the design is the allowable space in the model. Other constraints include the cost and time.

To be fast response, the junction between the two thermoelements must be minimised, To measure surface temperature the junction must be able to sit flush with the surface of the model without causing any interference to the flow. A cylindrically shaped thermocouple would simplify placement in the model and a flat end with a surface junction would allow surface measurement without disturbing the flow. An existing design, used in Buttsworth (2001), meets the shape requirements and was modified and employed. The thermoelements are in a co-axial arrangement, as illustrated in the diagram of the final design in figure 4.3. The surface junction could be created by using either a sharp object such as a scalpel to make a single score mark across the two materials or by using an abrasive paper to create many smaller junctions. The aim of the score or abrasion is to plastically deform the thermoelement material across the insulation and therefore create an electrical contact with the material on the other side.

Another method to simplify the design is to use normal signal wire rather than thermocouple extension wire. Extension wire is made from the same thermoelements in the thermocouple. The purpose of extension wire is to maintain homogeneity in each side of the thermocouple circuit so that the second electrical junction is at the voltmeter and the basic thermocouple circuit is preserved. If normal signal wire is used, the thermocouple circuit is changed. The effective circuit is shown in figure 4.1. The temperature measured is the temperature difference between T_1 and T_2, not T_3. This is because the signal wire is a homogeneous material, and the first law of thermocouples states that no emf is produced by a temperature change along a homegeneous section of the circuit. Therefore, the emf produced relates to the temperature difference between T_1 and T_2.

To enable the use of the thermocouples without extension wire, the thermocouples must be as long as possible so that the end opposite from the junction does not change temperature during the gun tunnel run.

In most applications, extension wire must be used rather than plain signal wire. Ex-

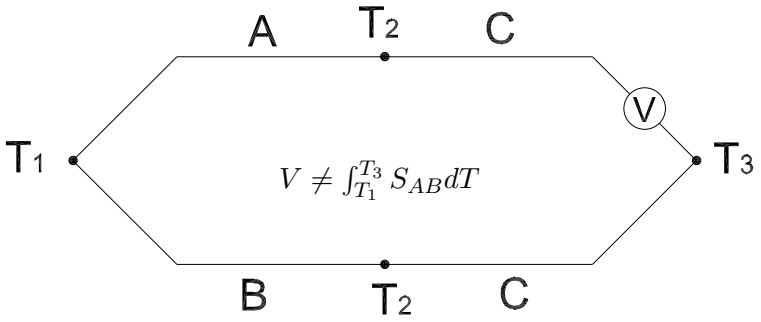

Figure 4.1: Typical thermocouple circuit without extension wire.

tension wire is not required in this design because the short period of high temperature flow in the gun tunnel and the length of the thermocouples allows the temperature at the end of the thermocouples, where the signal wire is soldered, to remain at constant temperature. The effective circuit produced is illustrated in figure 4.2.

There are numerous common thermoelements, resulting in a wide range of thermocouple combinations. The most common thermoelement combinations have been internationally standardised and are recognised by a lettering system. The standard combinations include E, T, J, K and S. The thermal product properties of selected thermoelements are displayed in Table 4.1

Variations between different thermocouples include temperature range, accuracy and corrosion resistivity. Variations are due to the individual physical properties of the thermoelements and and the properties of the thermocouple combination.

Type-E and K are the thermocouples most suitable for the temperature range and flow conditions of the gun tunnel. Type-E and type-K thermocouples share the same positive thermoelement and have similar temperature range, accuracy and resistance to corrosion. However, there are minor differences. Type-E has the highest emf per unit temperature change of all metal thermocouples and has a wider temperature range than type-K. Type-K thermocouples have a slightly higher resistance to corrosion than type-E.

Type-E thermocouples were decided for the project because type-E thermocouples are effective to higher temperature ranges than type-K and future work may involve the use of type-E thermocouples in internal combustion engines or other high temperature

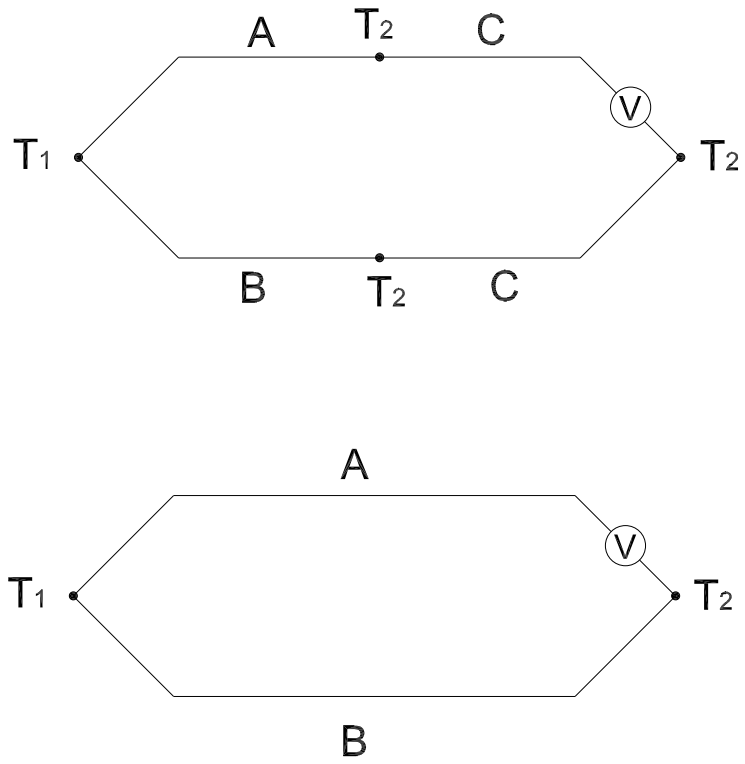

Figure 4.2: Top: Effective circuit in experiment; Bottom: Equivalent circuit.

applications. An aim of the project was to investigate the effectiveness of type-E thermocouples in the harsh conditions of the gun tunnel.

Type-E thermocouples are thermocouples that consist of chromel and constantan. Chromel is a positive thermoelement and its composition by weight is 89.9% nickel, 9.6% chromium plus other minor elements. Constantan is a negative thermoelement and its composition by weight is about 45% nickel, 55% copper plus small amounts of silicon, iron and manganese.

The final design is illustrated in figure 4.3. The thermocouple is co-axial with a chromel annulus 5 mm long and an outer diameter of 2.5 mm. A surface junction was created using emery paper. Signal wire was soldered to the wire and annulus while maintaining insulation, except for at the surface.

Table 4.1: Physical properties of common thermoelements.

Property	**Cu**	**NiCr (Chromel)**	**CuNi (Constantan)**	**Fe**	**NiAl (Alumel)**
Composition by weight		89.9% Ni 9.6%Cr	45% Ni55%Cu		95% Ni, 2% Al, 2% Mn, 1% Si
Density $\frac{kg}{m^3} \times 10^3$ at 0° C	8.9	8.8 to 8.9	8.5 to 8.6	7.85	8.7
Thermal Conductivity $\frac{W}{mK}$ at 0 to 300° C	389	40	15	75.3	58.6
Specific heat $\frac{J}{kgK}$ at 0 to 300° C	481	400	420	461	544

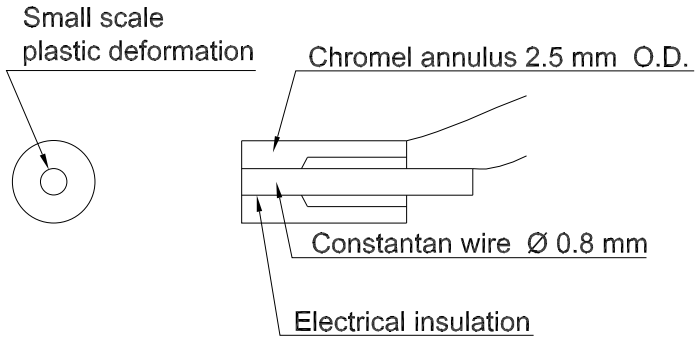

Figure 4.3: Design of thermocouple.

4.3 Construction

The bare thermocouple wires were purchased from Industrial Pyrometers by purchasing 5 m of 3.3 mm diameter type-K thermocouple material and 5 m of 0.8 mm diameter type-T material. The positive type-K material, chromel, is the positive type-E material and the negative type-T material, constantan, is the negative type-E material.

The thermocouple drawing, reproduced in Appendix B, was sent to the USQ workshop for machining. The annulus section was turned from an outside diameter of 3.3 mm to 2.5 mm. Holes were drilled to form an inside diameter of 0.8 mm for a depth of 2 mm and 1.5 mm for the remaining 3 mm. Twenty annulus sections were produced. The 0.8 mm inside diameter was widened slightly by hand to form a loose fit for the constantan wire. The wire was cut into 20 mm sections and then turned slightly with emery paper to help create a loose fit. A loose fit is required to allow an insulating oxide film to form between the surfaces. The process is described below.

The wire was sprayed with PCB lacquer to form an insulation before being inserted into the annulus. This was simply a temporary measure to insulate the thermoelements. A heat treatment oven was used to create a more permanent insulation. The high temperature allowed oxygen to react with the surface of the materials to create an insulating oxide film between the two materials. The thermocouples were placed in an oven at 650° C for six hours. After six hours the wires still were loose inside the annulus so they were baked for a further six hours. The oxide layer adds a small volume to the thermocouples and tightens the fit. The mass of the oxide film and the remnants of the PCB lacquer were assumed to have a negligible effect on the physical properties of the thermocouple.

Araldite was used to bond the wire to the annulus to prevent any movement. This was to ensure the surface junction was not affected and the insulation maintained elsewhere.

The constantan wire was trimmed to about 7 mm and insulated signal wire was soldered to the wire and annulus at the end opposite to the surface junction. The surface junction was formed using 120 grit emery paper.

4.4 Calibration

Calibration is required to take meaningful measurements from the thermocouples. While it is possible to read the Seebeck emf for E-type thermocouples from available charts and assume the gain of the amplifier as stated in its specification, it is more accurate to conduct a calibration experiment. The procedure is simple, accurate and takes little time.

An outline of the calibration procedure was as follows:

1. A thermocouple circuit was created by taking about 1 m of each E-type thermocouple wire and joining one end and wiring the other ends into the amplifier. The amplifier output was connected to a voltmeter to complete the circuit.
2. The junction was submerged in a water bath at various known temperatures while the length of the wire ensured that the other end remained constant at room temperature.
3. The output voltage at each temperature was recorded so that the difference in voltage between the known temperatures could be used to determine the voltage output per degree temperature change.

For the E-type thermocouples used, it was found through the calibration that 1 K temperature change produces 6.1 mV after amplification. Figure 4.4 is a diagram of the calibration procedure and figure 4.5 shows the results of the calibration. The calibration appears to be valid as the results show a linear correlation between temperature and voltage output and deviation from the regression line is small.

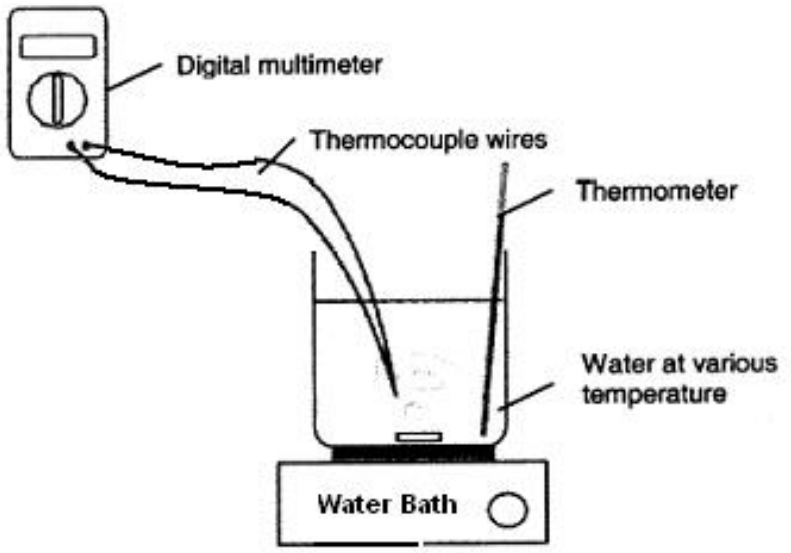

Figure 4.4: Calibration of the thermocouples (Laurel et al. 2002).

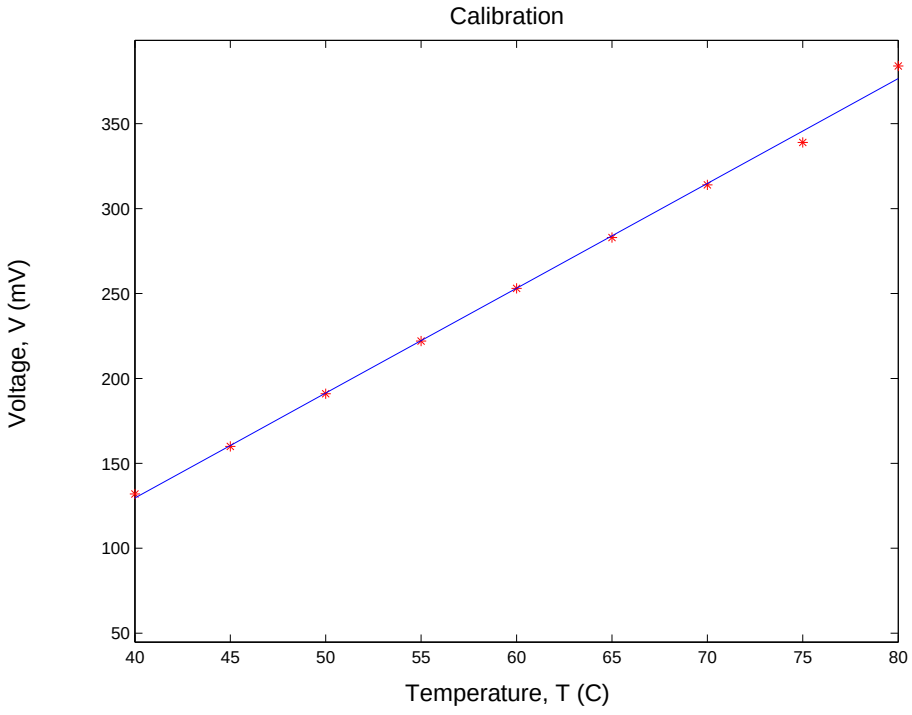

Figure 4.5: Results of the calibration.

4.5 Chapter Summary

The thermocouples were decided to be type-E and co-axial. A surface junction was created using emery paper. Signal wire was used to connect the thermocouples to the amplifier. Extension wire was not required because of the short duration of the heating.

The wire and annulus were machined at the USQ workshop and an insulating film was created by baking in a furnace. The heat of the furnace allows an oxide film to insulate the surfaces of the thermoelements.

The calibration was conducted by measuring the emf between known temperatures. The results of the calibration show that there was a strong accurate linear relationship between temperature change and voltage change. The calibration showed that the change in voltage with respect to temperature for the type-E thermocouples was 6.1 mV/K.

Chapter 5

Experimental Design

5.1 Chapter Overview

In this chapter, the aim, design and preparation of the experiment is discussed. This includes the design and construction of the Beagle 2 model, fitting the thermocouples in the model and fixing the model in the test section of the gun tunnel. It also includes a description of the equipment setup in preparation of the experiment.

5.2 Experiment Aim

The aim of this project was to investigate the effectiveness of type-E thermocouples at the measurement of heat transfer of a body in hypersonic flow. A thorough experimental programme would involve measuring the change of temperature at several positions on the wall of an entry capsule model in hypersonic flow so that heat flux could be determined. This would be achieved by placing thermocouples in the model and measuring the temperature change during the gun tunnel run. The aim of the experiment was to conduct at least one, but preferably four, gun tunnel runs so that there would be multiple results for each thermocouple. This would provide comprehensive results that would increase the credibility of the study.

5.3 Entry Capsule Model

The objective of the entry capsule model design was to create an accurate model of the Beagle 2 lander so that the thermal effects of re-entry could be simulated by the hypersonic flow of the gun tunnel. This included making the model diameter as large as possible so that the accuracy could be maximised and at least two thermocouples could be accommodated. It also included reproducing as much of the capsule shape beyond the front surface as possible.

The design was restrained by a number of factors. The model diameter was restricted by the exit nozzle of the gun tunnel. The nozzle diameter is 80 mm, so to ensure a stable cross-sectional flow across the surface of the model, taking into account boundary layer effects on the surface of the nozzle, the diameter of the model was restricted to 35 mm.

The objective to reproduce the dimensions beyond the front surface was restricted by the need for a backing plate to mount the model in the test section of the gun tunnel, as well as the need to provide space for the thermocouples and wire.

The drawings sent to the workshop for the final design are reproduced in Appendix B. The diameter is 35 mm and the rear section was only partially reproduced. The wall thickness was machined to 3 mm to allow the thermocouples to sit in the holes without the soldered ends preventing them from fitting. Three M3 holes were drilled in the back surface to attach the back plate. The back plate has a single M3 hole in the centre to attach to the jig in the test section.

The dimensions for the Beagle 2 lander were taken from Liever & Habchi (2003) and scaled down for 35 mm outer diameter. The drawings were sent to the USQ workshop where an aluminium model was machined.

Figure 5.1: Photograph of the Model. Thermocouples are seen sitting flush with the model surface.

5.4 Thermocouple in Model

The objective of the placement of the thermocouples was to position four thermocouples at different radii from the centre, at an angle perpendicular to the surface. The purpose of this was to analyse the heat transfer across the surface of the entry capsule as the shock layer thickened. An important part of the design was to ensure the thermocouples were flush with the surface to prevent any oblique shock effects. Another objective of the design was to insulate the thermocouples from the model. This would reduce background noise as well as prevent the thermocouples from interfering with each other.

The main restraint on the design was the limited space for the thermocouples. To overcome this restraint, two models were produced so that only two thermocouples would be required in each model while still covering all four positions.

The sides of the thermocouples were sprayed with PCB lacquer and inserted into the holes in the model. The resistance between the thermocouples and the model was tested to ensure insulation before araldite was used to hold them in place. When the araldite had set, a confirmatory check of the insulation showed that the insulation had failed. This may have been caused by slight movement prior to setting, causing part of the lacquer to scratch off. A picture of the thermocouples in the capsule model is illustrated in figure 5.1.

Figure 5.2: Photograph of the sting.

5.5 Model In Gun Tunnel

A system had to be designed to fix the model in the centre of the test section and to safely channel the thermocouple wires to the connections at the wall of the test section. A sting had already been designed by Terhorst (2001) and installed in the gun tunnel. It permits two degrees of freedom for the placement of the test piece. The test piece can be fixed at various angles of attack and different distances from the end of the nozzle. A picture of the sting is shown in figure 5.2.

Because there was no insulation between the thermocouples and the model, it was important that the model be insulated from the sting, and hence, the entire gun tunnel. This was achieved by applying duct tape to the backing plate on the surfaces normally in contact with the model. This meant that the M3 screws could no longer be used to hold the model to the backing plate. It was decided that the duct tape would be enough to hold the model in place because the model is axis-symmetrical and the angle of attack would be zero, therefore only an axial force would be present.

The wires were channelled to the wall by a piece of 3 x 25 mm mild steel that was bolted to the wall. The wires were run from the back of the model, along the rear of the steel bar and soldered to the connections in the wall.

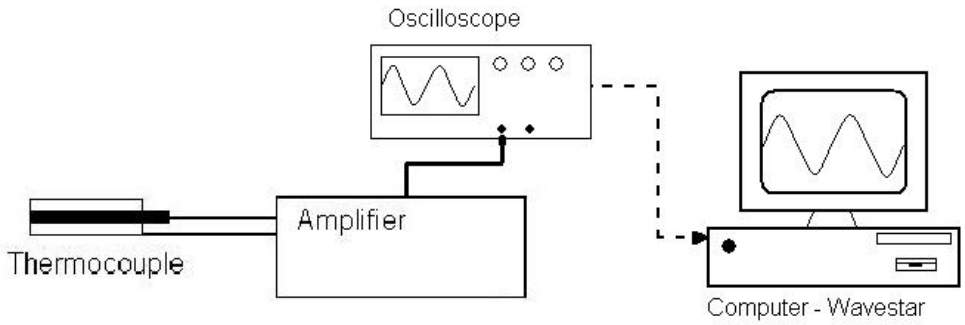

Figure 5.3: Recording the data.

5.6 Equipment Setup

The equipment was setup so that data could be easily recorded during the gun tunnel run. The signal from the thermocouple was connected into a thermocouple amplifier and the output from the amplifier was connected into an oscilloscope. A pressure transducer located at the end of the barrel was also connected into the oscilloscope so that stagnation pressure could be recorded. The pressure signal was used as the trigger for the oscilloscope. A flowchart of the process is shown in figure 5.3.

5.7 Chapter Summary

The thermocouples were installed in the entry capsule models so that temperature could be recorded at different radii from the centre. Unfortunately one of the objectives of the experimental design failed. There was no insulation between the thermocouples and the model. This meant that background noise would increase due to the model and greater noise would result if the model was fitted to the sting using the bolts. The method of fixing the model to the sting had to be modified.

Chapter 6

Results

6.1 Chapter Overview

The main objective of this project was to conduct heat transfer measurements of a re-entry capsule using fast response thermocouples and compare with existing theories of heat transfer. This chapter provides both the experimental and theoretical calculations, based on the results of the experiment. This chapter explains how the results were obtained, and the following chapter analyses the results.

6.2 Converting Signals into Temperature and Pressure

After the gun tunnel run, the data from the oscilloscope was downloaded onto a computer where it was converted into a `.txt` file using wavestar, the software that is used for the oscilloscope. The text file was converted into a valid `.m` MATLAB data file using `load_wavestar_2.m`, a MATLAB script by Buttsworth (script is reproduced in Appendix C). The values in the data file were converted to temperature and pressure using the results of the calibration. Formatted values of pressure and temperature change are plotted against time in figure 6.1 and figure 6.2.

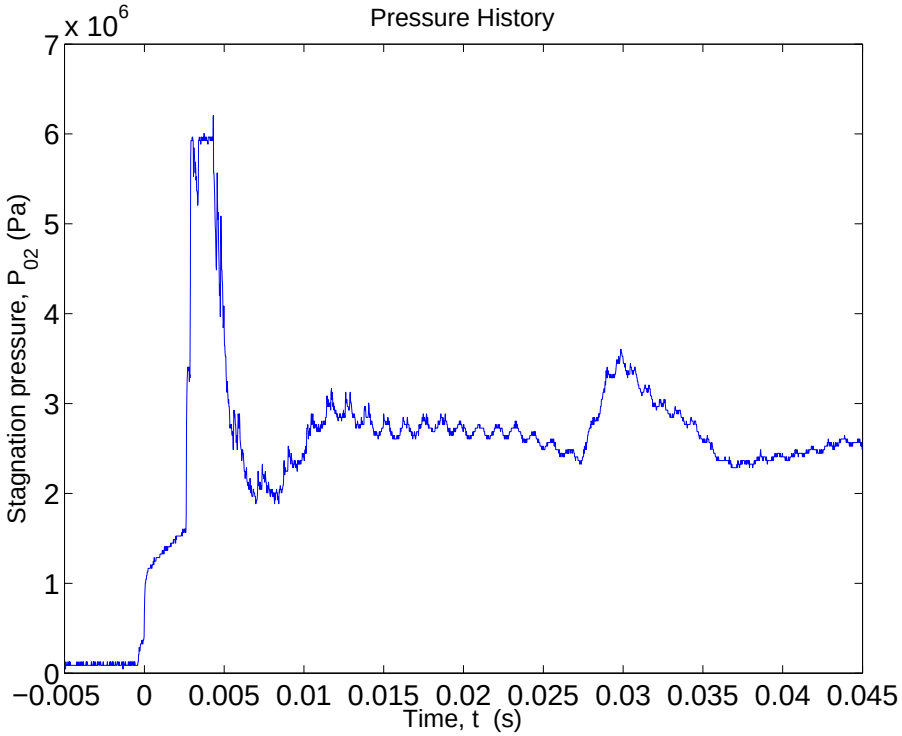

Figure 6.1: Pressure history from experiment.

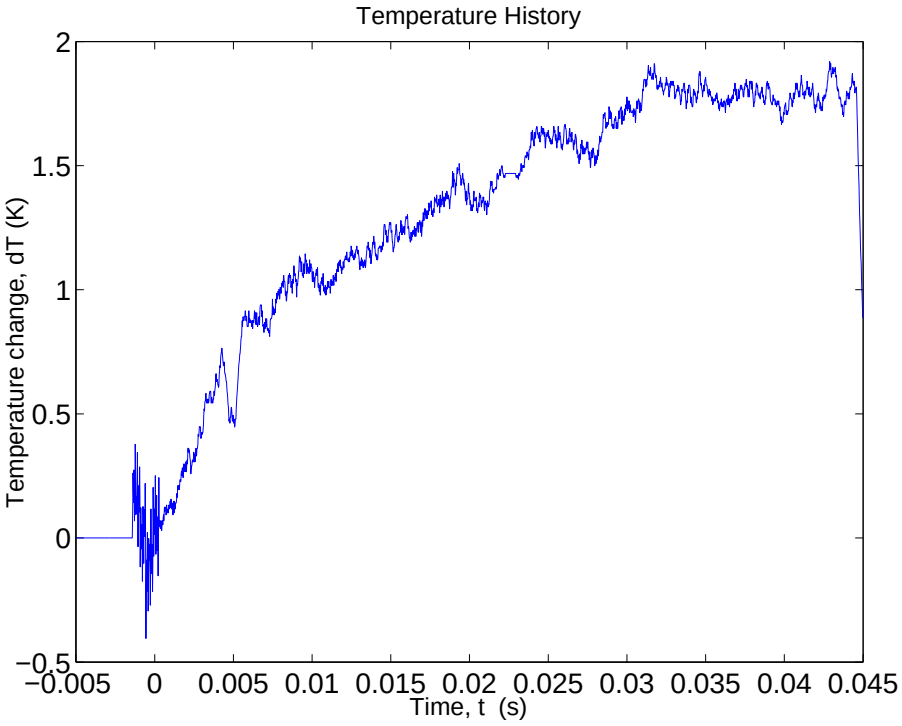

Figure 6.2: Temperature history from experiment.

6.3 Calculating Heat Flux from Temperature Change

Experimental results were calculated using the Cook-Felderman method as cited in Hollis & Perkins (1996). The Cook-Felderman method calculates the one-dimensional heat conduction, assuming a flat plate. It is designed for wind tunnel testing because it uses the temperature history and time history vectors as inputs. The Cook-Felderman method is described mathematically as:

$$q'' = \frac{2\beta}{\sqrt{\pi}} \sum_{i=1}^{i=n} \frac{T_i + T_{i-1}}{\sqrt{t_n - t_i} + \sqrt{t_n - t_{i-1}}} \tag{6.1}$$

where T is the temperature change, t is time and β is the thermal product of the thermocouple, $\beta = \sqrt{\rho c_p k}$. A MATLAB script of this method is reproduced in Appendix C. This method assumes constant thermal properties. This can be expected as the temperature of the wall only changes by 2° K. This method also assumes a flat plate. A modified version of this method was written by Buttsworth, also in Appendix C, and includes a correction factor for curved surfaces. Comparison of the two scripts revealed that the correction factor made little difference in the results. A plot of the heat transfer using the Cook-Felderman method is displayed in figure 6.3. The plot is a smoothed version of the actual data because the raw temperature data had a large amplitude noise and spikes. Before calculating heat transfer, the temperature history was formatted. The large spikes, caused by unknown interference, were removed and the data points were replaced with the average of the points before and after the spike. The temperature history was also smoothed to remove some of the noise.

The heat flux history was averaged across the effective section of the plot. The effective section was the region of stable pressure from $t = 0.010$ to $t = 0.027$ ms. The average heat flux across that region was 82 kW/m^2.

6.4 Calculating Heat Flux from Theory

A theoretical value for heat flux was calculated using equation 6.2:

$$Nu = 0.736 Pr^{0.4} Re^{0.5} C^{0.1} \left(\frac{KD}{U_\infty}\right)^{0.5} \tag{6.2}$$

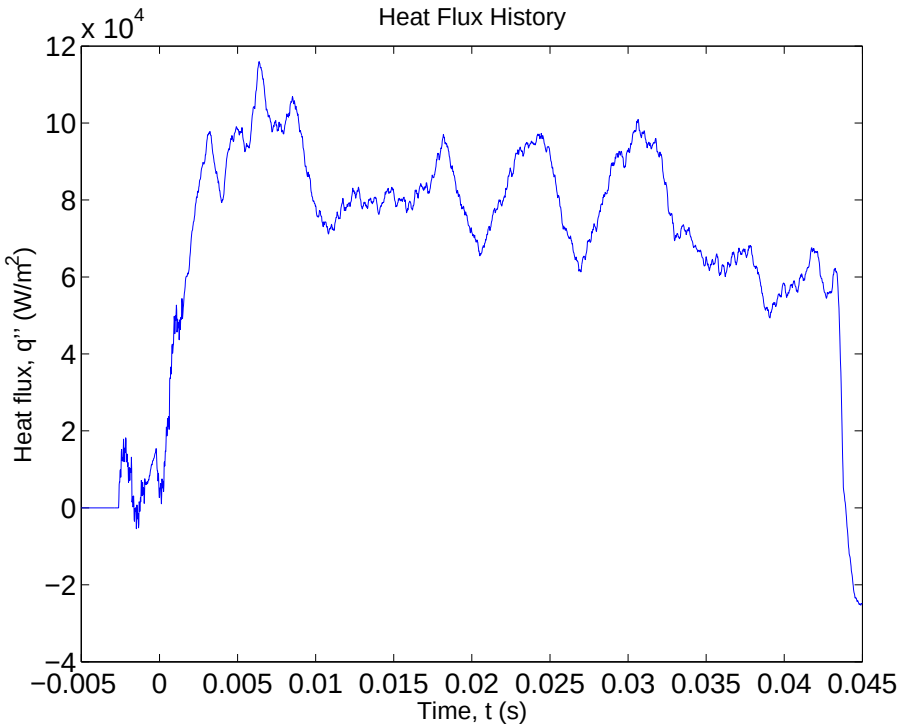

Figure 6.3: Smoothed heat flux.

where

$$
\begin{aligned}
Nu &= \frac{h_c D}{k} \\
Pr &= \frac{c_p \mu_{02}}{k_{02}} \\
Re &= \frac{\rho_{02} U_\infty D}{\mu_{02}} \\
K &= \frac{du_{02}}{dx} \\
C &= \frac{\rho_w \mu_w}{\rho_{02} \mu_{02}}
\end{aligned}
$$

To use these series of equations, physical properties of the flow, such as density, pressure, temperature, viscosity, specific heat and conduction heat transfer coefficient must be known at free stream, stagnation and wall conditions. The known properties are shown in table 6.1. The properties measured during the gun tunnel run are shown in table 6.2. The remaining properties shown in table 6.3 must be calculated from fluid mechanics theory.

The initial pressure and temperature were the laboratory conditions at the time of testing. Pressure was assumed to be the standard atmospheric pressure for Toowoomba

Table 6.1: Known properties.

Initial Pressure	P_i	94000 Pa
Initial Temperature	T_i	288 K
Specific Heat Capacity	c_p	1044 J/(kg.K)
Specific Heat Ratio	γ	1.4

Table 6.2: Measured properties.

Average Stagnation Pressure	P_0	2.7 MPa
Maximum Temperature Change	dT	1.75 K

and temperature was measured using a thermometer. Specific heat capacity for constant pressure and the specific heat ratio was assumed to be constant at 1044 J/(kg.K) and 1.4 respectively. These values vary about 8.0% between free stream conditions and stagnation conditions. An average of the two was used for the analysis.

The average stagnation pressure was determined by studying the plot of the stagnation pressure history, shown in figure 6.1. The flow is assumed to be isentropic and therefore the stagnation pressure measured at the end of the barrel is the same at the test section. The relatively flat section after the initial spike was considered the stable period of the flow. It lasts for about 17 ms which is typical for the gun tunnel. The mean of the stagnation pressure during this period was used for the average stagnation pressure.

Stagnation Temperature, T_0, was calculated by assuming isentropic compression from

Table 6.3: Calculated properties.

Stagnation Temperature	T_{01}	$751K$
Free Stream Temperature	T_∞	$72.7K$
Free Stream Pressure	P_∞	$572Pa$
Free Stream Density	ρ_∞	$0.0274kg/m^3$
Stagnation Temperature after shock	T_{02}	$751K$
Stagnation Pressure after shock	P_{02}	$35.98kPa$
Stagnation Density after shock	ρ_{02}	$0.167kg/m^3$
Stagnation Viscosity after shock	μ_{02}	$3.48kg/(s.m)$
Stagnation Thermal Conductivity after shock	k_{02}	$0.0475W/(m.K)$
Density at the wall	ρ_w	$0.435kg/m^3$
Viscosity at the wall	μ_w	$1.789kg/(s.m)$
Thermal Conductivity at the wall	k_w	$0.0244W/(m.K)$

initial conditions prior to the gun tunnel run to the high pressure stagnation conditions:

$$T_0 = T_i R \left(\frac{P_i}{V_0}\right)^{\gamma} \tag{6.3}$$

Free stream temperature, T_∞, and free stream pressure was calculated by assuming isentropic compressible flow. Isentropic flow is dependant on the Mach number, M, and the ratio of specific heats, γ, and is represented by the following functions:

$$\frac{T_{01}}{T_\infty} = 1 + \frac{\gamma - 1}{2} M^2 \tag{6.4}$$

$$\frac{P_{01}}{P_\infty} = \left[1 + \frac{\gamma - 1}{2} M^2\right]^{\frac{\gamma}{\gamma - 1}} \tag{6.5}$$

The entry capsule was subjected to a hypersonic flow at zero angle of attack and therefore the shock wave can be assumed to be normal shock conditions. Hence, Normal shock flow functions were used to calculate stagnation pressure downstream from the shock wave:

$$\frac{P_{02}}{P_{01}} = \frac{\left[\frac{\frac{\gamma+1}{2} M_\infty^2}{1 + \frac{\gamma-1}{2} M_\infty^2}\right]^{\frac{\gamma}{\gamma-1}}}{\left[\frac{2\gamma}{\gamma+1} M_\infty^2 - \frac{\gamma-1}{\gamma+1}\right]^{\frac{1}{\gamma-1}}} \tag{6.6}$$

The flow was assumed to be an ideal gas, shown in equation 2.1 and the density at all conditions was calculated based on that assumption.

Thermal conductivity and absolute viscosity are dependant on temperature and don't vary much with pressure within the temperature range of the gun tunnel. Sutherland developed equations for conductivity and viscosity as a function of temperature and is cited in Bertin (1994). The correlations are accurate for the temperature range in the gun tunnel and hence were used to calculate viscosity and thermal conductivity at all flow conditions:

$$\mu = 1.458 \times 10^{-6} \frac{T^{1.5}}{T + 110.4} \tag{6.7}$$

$$k = 1.993 \times 10^{-5} \frac{T^{1.5}}{T + 112} \tag{6.8}$$

$\frac{KD}{U_\infty}$ was calculated by the approximation

$$\frac{KD}{U_\infty} \approx \left(\frac{8\rho_\infty}{\rho_{02}}\right)^{0.5} \; for\; M_\infty > 1.2 \tag{6.9}$$

as cited in Buttsworth & Jones (2003).

Substituting the above values into equation 6.2 gives the Nusselt number for the period of stable stagnation pressure. The Nusselt number can also be expressed as:

$$Nu = \frac{h_c D}{k_w} \tag{6.10}$$

to find the heat transfer coefficient at the wall. The heat transfer at the wall was calculated using the standard convection heat transfer equation:

$$\begin{aligned} q'' &= h_c(T_{02} - T_w) \\ q'' &= 104 \;\; kW/m^2 \end{aligned} \tag{6.11}$$

6.5 Chapter Summary

Experimental results were obtained by using the Cook-Felderman method. This method requires the temperature and time history vectors and the thermal product of the thermocouples. The raw temperature data had high amplitude noise and spikes that had to be removed before reasonable results could be achieved. The average experimental heat flux was found to be 82 kW/m^2.

The theoretical results were calculated using a correlation by White (1991). It was used to calculate the Nusselt number so that the convection heat transfer coefficient could be found and, hence, heat flux could be derived. The correlation required the calculation of numerous parameters at free stream, stagnation and wall conditions. These values were calculated from the known and measured properties. 10 kw/m^2 was the heat flux calculated from theory.

Chapter 7

Discussion

7.1 Chapter Overview

This chapter presents an analysis of both the experimental and theoretical results and discusses the differences between them. The analysis involves a discussion of the assumptions associated with each of the results as well as the causes of uncertainty and the problems that arose during the experiment. The comparison of the results includes comments about the credibility of the results and affirms the validity of the study.

7.2 Theoretical Results

7.2.1 Assumptions

The theoretical results were based on many assumptions. Most of the assumptions were accurate but other assumptions were made because there was no better alternative.

The first major assumption was in the equation to determine the Nusselt number, equation 6.2. The assumption is that the object is a sphere. This assumption was made because of the lack of a better alternative. There were no heat flux correlations designed for the Beagle 2 dimensions. All existing heat flux predictions for the Beagle

2 were calculated using complex Computational Fluid Dynamics (CFD) routines. The closest existing correlations for a re-entry vehicle were for a flat plate or for a sphere.

It can be seen in table 6.3 that there were many parameters to be calculated using theory, in order to calculate the theoretical heat flux. Each calculation was based on an assumption or series of assumptions. To calculate stagnation temperature, isentropic expansion and compression were assumed from atmospheric pressure to low pressure partial evacuation to high pressure stagnation conditions during the gun tunnel run.

Isentropic flow was assumed to calculate free stream temperature and pressure from stagnation temperature and pressure. This was expected to be an accurate assumption since the test time was short.

The conditions at the wall were assumed to be constant. The thermocouple indicated that there was a maximum temperature change of 2 K. It was therefore reasonable to assume constant temperature to calculate the wall density and pressure.

The thermal conductivity and absolute viscosity were calculated using Sutherland correlations. These correlations assume the property is not affected by change in pressure. Anderson (1989) states that the Sutherland equations are accurate at low pressure and at temperatures up to about 1500 K. The maximum pressure and temperature that viscosity and thermal conductivity were calculated at was 36 kPa and 751 K respectively. Therefore the assumption was reasonable.

The most important assumption was for the values of specific heat and the ratio of specific heats. The heat flux was very sensitive to a change in these properties. There is a 3% variance between the stagnation specific heat ratio and the free stream specific heat ratio. This variance causes a 17% difference in the heat flux. The specific heat ratio is used in the isentropic flow functions, normal flow functions and for determining the speed of sound. For the normal flow functions and speed of sound, the specific heat ratio appropriate to the temperature involved could be used. However for the isentropic flow functions, both temperatures are involved, so an average value was used.

7.2.2 Uncertainty

Uncertainty in the theoretical results is due to the assumptions required to calculate all of the parameters. Also, the equation used for the results assumes a spherical geometry, which would affect the results.

7.3 Experimental Results

7.3.1 Assumptions

The Cook-Felderman method computes heat flux for one-dimensional, semi-infinite, flat plate conduction. The thermocouple was positioned in the centre and the heat acted on one surface only, therefore, it is reasonable to assume one dimensional heat conduction.

The Cook-Felderman method assumes a constant thermal product. Hollis & Perkins (1996) uses a correction factor to eliminate the problem but, in this project the wall temperature only changes by about 2° K so the thermal product would not change.

7.3.2 Problems Encountered

The aim of the project was to investigate the effectiveness of type-E thermocouples in measurement of hypersonic heat transfer. The aim of the experiment was to provide comprehensive and credible results for analysis. There were numerous problems that prevented complete and thorough results.

When fitting the thermocouples in the model, the aim was to ensure that insulation was maintained between the thermocouples and the model. This was to minimise the noise from the model and gun tunnel and to prevent interference from the other thermocouple. This aim was not achieved and therefore the design of the experiment had to be modified. The model was insulated from the sting and, hence the gun tunnel so that noise could be minimised.

The thermocouples were connected to the amplifier using signal wire. The wire is fragile and a lot of time was spent re-soldering broken connections. This was a time consuming exercise that could have been avoided by taking extra care during handling of the thermocouples and by using thicker wire.

Due to time restraints, only one gun tunnel run was conducted. During the preparation for that run, the wires were broken from one of the thermocouples while fitting the model in the test section. It was decided that the run would be conducted with just the single thermocouple. Therefore, there was only one set of results for one thermocouple.

7.3.3 Uncertainty

Error can be attributed to a number of factors. The background noise in the temperature history generates a level of uncertainty and the spikes in the data compounds the error. Any surface defects would also affect the temperature history data as a disturbance would affect the flow. The thermocouple must be flush with the surface and must not move during the test time.

The thermal product, β, of the thermocouples was required for the calculation of heat flux. It was calculated using standard values of density, specific heat and thermal conductivity. However, Buttsworth (2001) found in his work with type-K thermaocouples that the thermal product varies considerably from gauge to gauge when a surface junction is created using abrasive paper. This is a result of the effect of the insulating film between the thermoelements. Chromel and constantan have similar thermal products but to accurately estimate the total thermal product of the junction, the thermal product of the insulating film must be taken into account.

7.4 Comparison of Experimental and Theoretical Results

The theoretical results predicted an average heat flux of 104 kW/m^2 and the experiment produced an average heat flux of 82 kW/m^2 during the stable period of the flow. A plot of the theoretical and experimental results during the effective test time, are shown in

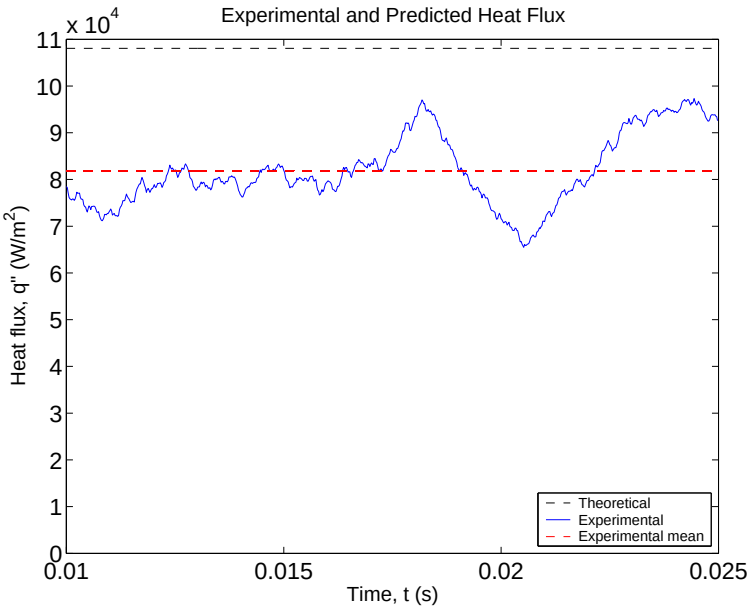

Figure 7.1: Comparing experimental heat flux with theoretical prediction.

figure 7.1.

Both results contain a high level of uncertainty, therefore, neither can be viewed as the right answer to which the other is compared. However, the fact that the results are within 20% of each other is reasonable considering the minimal experimentation involved.

It is clear that the results do not provide a complete insight into the effectiveness of type-E thermocouples in the measurement of heat transfer of an object in hypersonic flow. The results had excessive noise and uncertainty in the accuracy of the thermal product. The predicted result had a high level of uncertainty due to the amount of assumptions. It does provide, however, a platform for future work to complete the study.

While the results do not provide an informative heat transfer prediction for heat shield design, it does provide evidence that further work in this area is valid. A detailed discussion of further work is presented in the next chapter.

7.5 Chapter Summary

The theoretical prediction was based on numerous assumptions and the experimental results had excessive noise and a thermal product of unknown accuracy. In light of this, the experimental and predicted results were within 20% of each other. While this does not provide a clear indication of the effectiveness of type-E thermocouples, it does validate future work in this area, in order to complete the study.

Chapter 8

Conclusions and Further Work

8.1 Achievement of Project Objectives

The aim of the project was to investigate the application of fast response thermocouples to measurement of heat transfer in the hypersonic flow produced by the gun tunnel and obtain representative data on a selected capsule geometry for comparison with theory or other experiments. This was achieved by conducting background research, an experiment and analysis of the results.

The background research was divided into four categories:

1. Hypersonic convection heat transfer;
2. Re-entry vehicles;
3. High speed wind tunnels; and
4. Temperature measurement systems.

In order to review hypersonic convection heat transfer, it was necessary to first research hypersonic flow and convection heat transfer. The review of hypersonic heat transfer included pioneer heat transfer theories from the 1950's to more recent theories that require numerical methods to solve. The study of re-entry capsules gave an introduction

into the roles and various types of entry vehicles. The review of gun tunnels included a brief background study into the history and the various types of high speed wind tunnels. However, the review concentrated on the USQ gun tunnel. Part of the project aim is to investigate fast response thermocouples, so the background research included a brief review of thermocouples and other temperature measurement systems.

An experiment was designed to apply fast response thermocouples to the measurement of heat transfer in hypersonic flow. Suitable construction techniques were employed to produce fast response thermocouples, capable of measuring the change in temperature of the model wall during the test time of a gun tunnel run. One-dimensional heat conduction was assumed to calculate the heat flux history, using the temperature history data as step inputs for direct calculation. The experimental heat flux was compared with a theoretical prediction using a heat transfer model by White (1991), cited by Buttsworth & Jones (2003). While the results were far from ideal, the objectives were achieved and the study provides a platform for future work.

8.2 Further Work

There is potential for a variety of future work associated with this project. The further work of this study can be divided into two areas:

- The work required to complete the aim of the investigation, and
- The future applications for heat transfer measurements using fast response thermocouples.

The work required to complete the aim of the investigation is the work that would have been conducted in this project, had there been more time. The work includes revising the design of the experiment and conducting a more comprehensive experimental programme.

There are several modifications to the experiment that could improve the credibility of the results. The thermocouples must be insulated from the model. This could

be achieved by either constructing the model using a nonconducting material or by improving the insulation technique. Other methods of creating a surface junction and insulating film could be tested to improve the prediction of the thermal product. More informative results could be analysed to compare with heat transfer predictions at actual entry conditions.

Future heat transfer measurements using fast response thermocouples could include a range of applications. A suggested application is to install thermocouples in an internal combustion engine. The thermocouples could be inserted into the head or the cylinder wall. With thermocouples located at different points in the cylinder, comprehensive temperature history data could be produced. This could give insight into the performance of the cooling system and the distribution of the combustion. The current study has shown that type-E thermocouples are capable of providing temperature measurements in harsh hypersonic flow conditions for short time scales. The application of type-E thermocouples in an internal combustion engine would provide an assessment of the thermocouples at high temperature and pressure conditions for longer durations.

8.3 Conclusions

The experiment provided heat transfer data of a small scale Beagle 2 entry capsule based on temperature history data of the model wall produced by fast response, type-E thermocouples. The results were compared with theoretical results based on a hypersonic convection heat transfer correlation by White (1991). The results were reasonable, considering the assumptions and uncertainty in both predictions.

This project has provided evidence that there is potential for the application of type-E thermocouples in the measurement of heat transfer in the hypersonic flow produced by a Mach 7 gun tunnel. Further work is required to provide a more comprehensive assessment of this potential.

References

Anderson, J. D. (1989), *Hypersonic and High Temperature Gas Dynamics*, McGraw Hill, USA.

Baals, D. & Corliss, W. (1981), *Wind Tunnels of NASA*, World Wide Web, http://www.hq.nasa.gov/office/pao/History/SP-440/cover.htm.

Beagle 2: A Brittish Led Exploration of Mars (2004), World Wide Web, `www.beagle2.com`.

Bedford, R. E. (1990), Physical priciples, *in* W. Göpel, J. Heese & J. N. Zemel, eds, 'Sensors - A Comprehensive Survey - Thermal Sensors', Vol. 4, VCH Publishers, New York, USA.

Bertin, J. J. (1994), *Hypersonic Aerothermodynamics*, AIAA, USA.

Blake, O., Bridges, J., Chester, E. & et al (2004), Beagle 2 mars mission report, Technical report.

Buttsworth, D. (2001), 'Assessment of effective thermal product of surface junction thermocouples on millisecond and microsecond time scales', *Experimental Thermal and Fluid Science* **vol. 25**, pp409–420.

Buttsworth, D. & Jacobs, P. (1998), 'Total temperature measurements in a shock tunnel facility', *13th Australian Fluid Mechanics Conference, Monash University* .

Buttsworth, D. & Jones, T. (2003), 'Concentration probe measurements in a mach 4 nonreacting hydrogen jet', *Journal of Fluids Engineering* **vol. 125**, pp 628–635.

Eckert, E. & Goldstein, R. (1976), *Measurements in Heat Transfer*, Hemisphere Publishing Corporation, USA.

Fox, R. & McDonald, A. (2004), *Introduction to Fluid Mechanics*, John Wiley and Sons.

Hankey, W. (1988), *Re-entry Aerodynamics*, AIAA, USA.

Hollis, B. & Perkins, J. (1996), Hypervelocity heat transfer measurements in an expansion tube, *in* '19th AIAA Advanced Measurement and Ground Testing Technology Conference'.

Kreith, F. & Bohn, M. S. (2001), *Principles of Heat Transfer*, Brooks/Cole, USA.

Laurel, I., Morgan, R. & Buttsworth, D. (2002), 'Fast response co-axial type-e themocouple gauges for the measurement of heat flux in expansion tubes', *Mechanical Engineering Research Report* (No. 2001/05).

Liever, P. & Habchi, S. (2003), 'Computational fluid dynamics predicition of the beagle 2 aerodynamic database', *Journal of Spacecraft and Rockets* **vol. 40**(No. 5), pp 635–638.

Mars Exploration Rover Mission (2004), World Wide Web, `http://marsrovers.jpl.nasa.gov/home/index.html`.

McGee, T. D. (1988), *Principles and Methods of Temperature Measurement*, John Wiley and Sons, USA.

Meese, E. & Nørstrud, H. (2002), 'Simulation of convective heat flux and heat penetration for a spacecraft at re-entry', *Aerospace Science and Technology* **vol. 6**, pp 185–194.

Michalski, L., Eckersdorf, K. & McGhee, J. (1991), *Temperature Measurement*, John Wiley and Sons, Great Brittain.

Pope, A. (1954), *Wind Tunnel Testing*, John Wiley and Sons, USA.

Pope, A. & Goin, K. (1965), *High Speed Wind Tunnel Testing*, John Wiley and Sons, USA.

Terhorst, J. (2001), Aerodynamic force measurement system for the usq gun tunnel, Master's thesis, University of Southern Queensland.

Vanvor, H. (1990), Thermocouples, *in* W. Göpel, J. Heese & J. N. Zemel, eds, 'Sensors - A Comprehensive Survey - Thermal Sensors', Vol. 4, VCH Publishers, New York, USA.

Appendix A

Project Specification

University of Southern Queensland
Faculty of Engineering and Surveying

Eng4111/4112 Research Project
PROJECT SPECIFICATION

FOR: **Brody ROACHE**

TOPIC: HEAT TRANSFER MEASUREMENTS OF A RE-ENTRY CAPSULE USING FAST RESPONSE THERMOCOUPLES

SUPERVISOR: Dr. David Buttsworth

PROJECT AIM: This project aims to investigate the application of fast response thermocouples to the measurement of heat transfer in the hypersonic flow produced by the gun tunnel, and obtain representative data on selected re-entry capsule geometries for comparison with theory and other experiments.

PROGRAMME: Issue A, 24 March 2004

1. Literature work (a) – review existing theories for convective heat transfer on aerodynamic entry capsules.
2. Literature work (b) – identify relevant geometries of existing and proposed capsules from the literature.
3. Literature work (c) – identify important previous experiments on capsule heat transfer (either wind tunnel or flight).
4. Review operation of gun tunnel, fast-response thermocouples (K or E-type), and other related instrumentation.
5. Develop suitable construction techniques for E-type thermocouples.
6. Design and perform experiments in gun tunnel on a capsule geometry.
7. Analyse heat transfer data and compare with existing theories and/or other experiments.

As time permits

8. Repeat 6 and 7 above for other relevant geometries.

AGREED:_____(Student) _____(Supervisor)

(Dated) ____/____/____

Appendix B

Technical Drawings

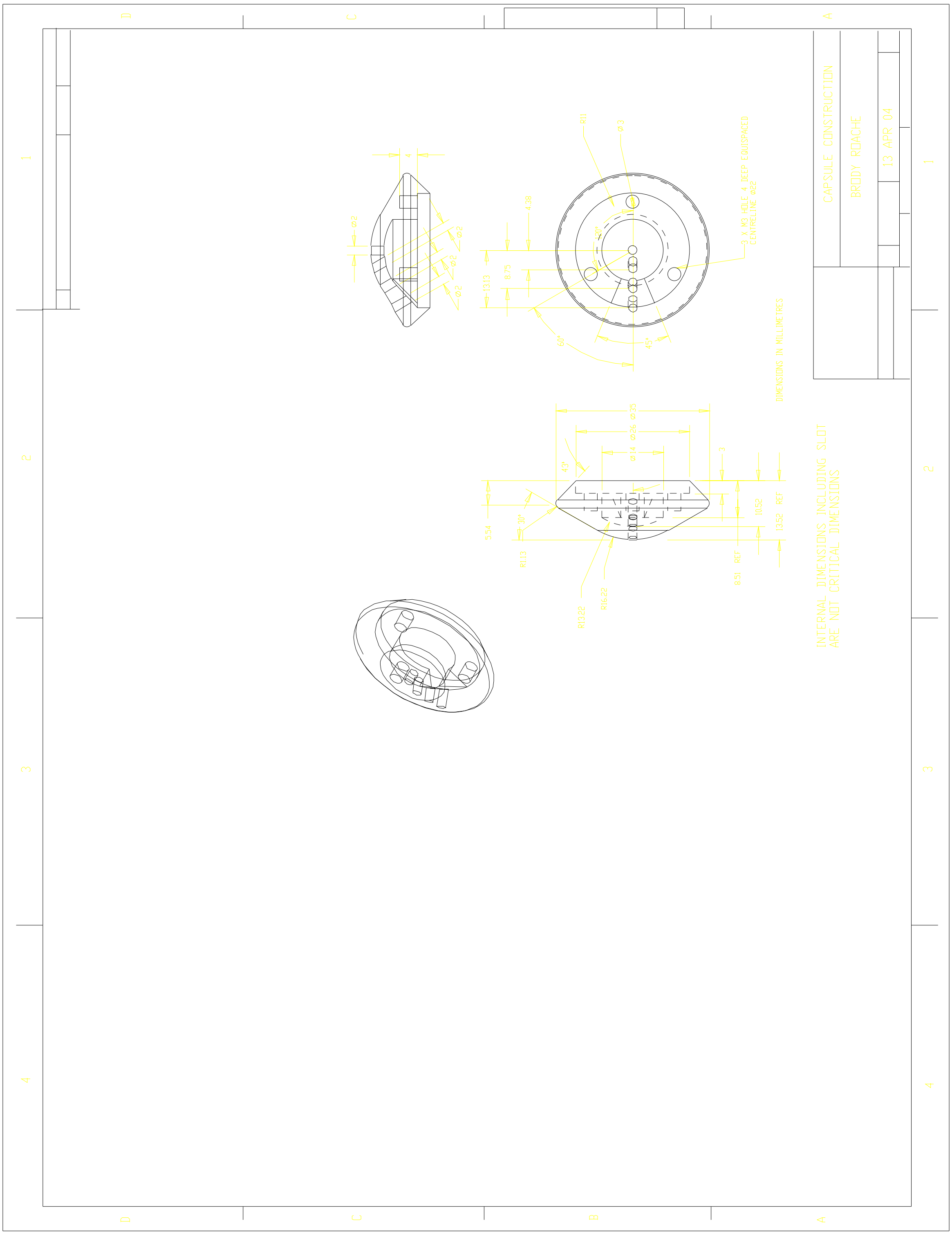
CAPSULE CONSTRUCTION
BRODY ROACHE
13 APR 04
3 X M3 HOLE 4 DEEP EQUISPACED
CENTRELINE Ø22
DIMENSIONS IN MILLIMETRES
INTERNAL DIMENSIONS INCLUDING SLOT
ARE NOT CRITICAL DIMENSIONS
10.52
13.52 REF

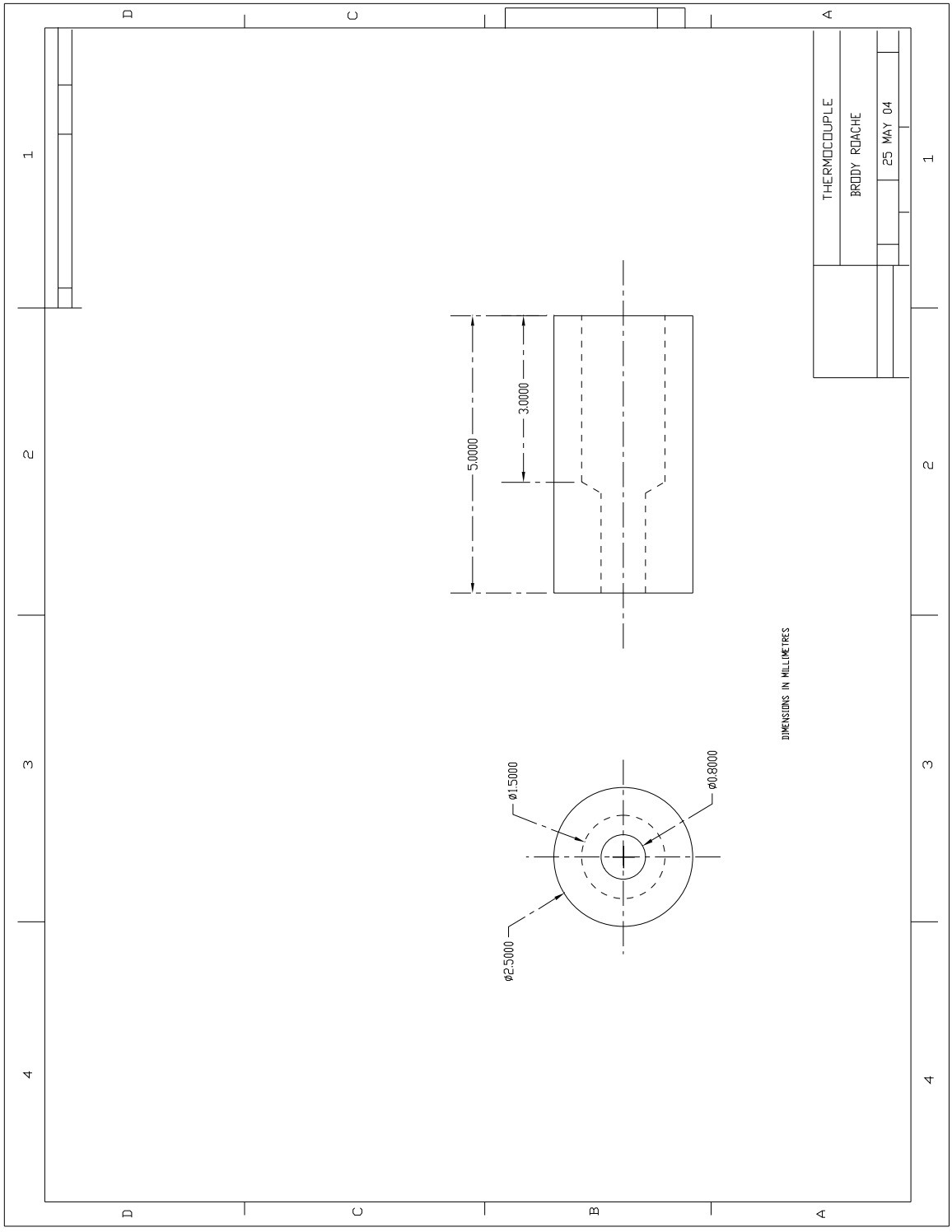
THERMOCOUPLE
BRODY ROACHE
25 MAY 04
5.0000
3.0000
ø1.5000
ø0.8000
ø2.5000
DIMENSIONS IN MILLIMETRES

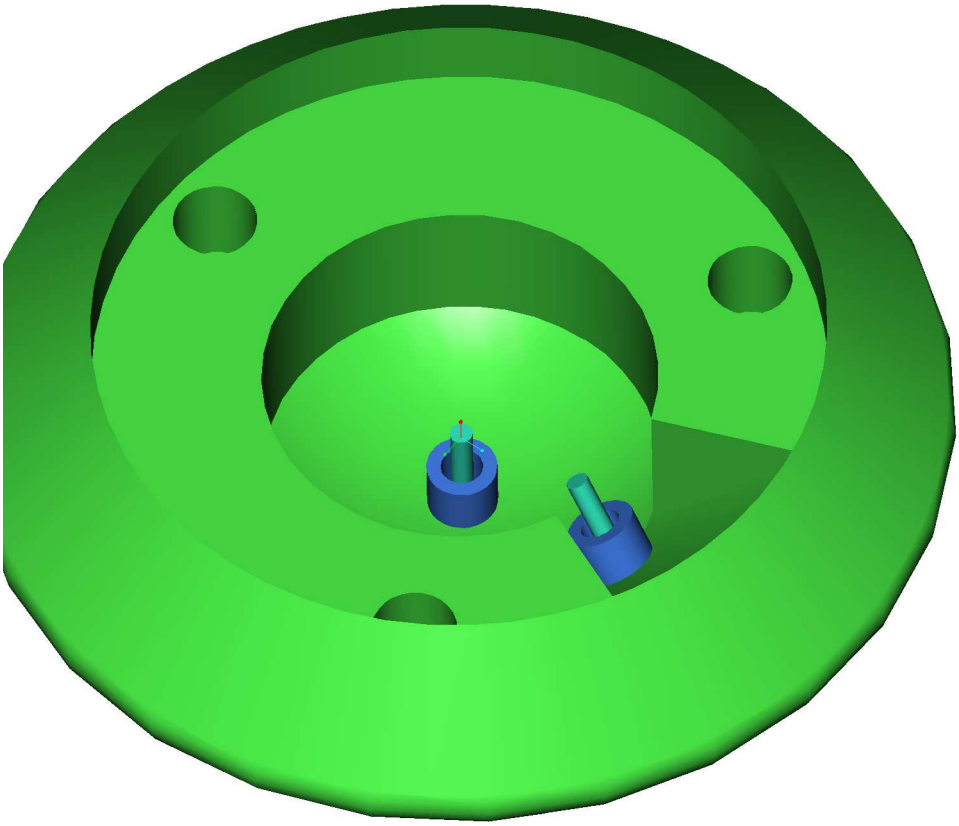

Figure B.1: Back view of the thermocouples in the Beagle 2 model

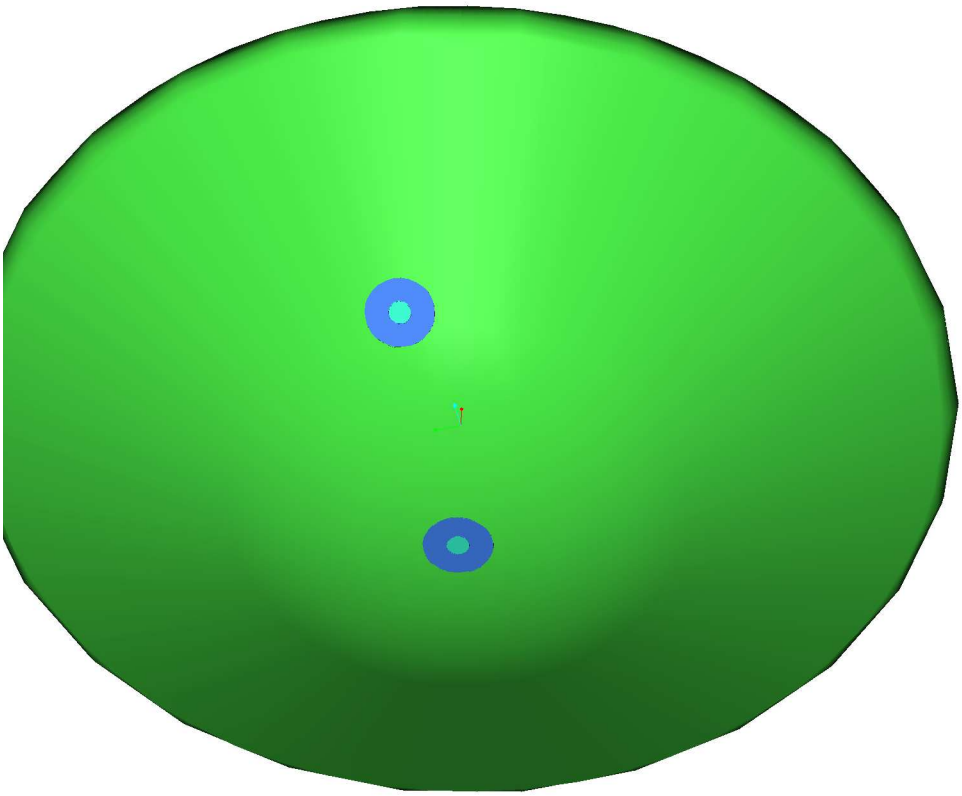

Figure B.2: Front view of the thermocouples in the Beagle 2 model

Appendix C

MATLAB Code

C.1 Wavestar to MATLAB Conversion (load_wavestar_2.m)

This function converts a `.txt` file from Wavestar into a valid MATLAB matrix, stored as a `.m` file. Script by David Buttsworth.

```
function data=load_wavestar_2(file_name,nrows,ncolumns);

fid=fopen(file_name);

fscanf(fid,'%s',ncolumns)

for i=1:nrows,
    i
    for j=1:ncolumns,
        num1=fscanf(fid,'%f',1);
        char1=fscanf(fid,'%s',1);
        if char1=='m',
            data(i,j)=num1*1e-3;
            fscanf(fid,'%s',1);
        elseif char1=='u',
            data(i,j)=num1*1e-6;
            fscanf(fid,'%s',1);
        elseif char1=='n',
            data(i,j)=num1*1e-9;
            fscanf(fid,'%s',1);
        else
            data(i,j)=num1;
        end
    end
end

st=fclose(fid);
```

C.2 Main Script (gt37analysis.m)

```
%%%%%%%%%%%%%%%%%%%%%%%%%%%%%%%%%%%%%%%%%%%%%%%%%%%%%%%%%%%%%%%%%%%%%%%%%%%%
%
%This script loads the matrix, gt37, and calculates the experimental and
%theoretical heat flux. Pressure, temperature and heat flux plots are
%created.
%       Brody Roache    2004
%%%%%%%%%%%%%%%%%%%%%%%%%%%%%%%%%%%%%%%%%%%%%%%%%%%%%%%%%%%%%%%%%%%%%%%%%%%%
%
load gt37;
tim=gt37(:,1);
stg=gt37(:,4);
tc=gt37(:,2);


nzero=[1:200]';

% stagnation pressure - actual units
stg_sens=1e-6;                      %pressure transducer sensitivity V/Pa
stg=(stg-mean(stg(nzero)))/stg_sens+94e3;
                                    %stg = absolute pressure
                                    %stg(nzero)= first 200 points -
                                    % initial condition


%Surface Temperature change - actual units
tc_sens=-0.00617;                   %Thermocouple sensitivity -
                                    %from calibration V/K
tc=(tc-mean(tc(nzero)))/tc_sens;    %tc = change in temperature
                                    %tc(nzero)= first 200 points -
                                    %initial condition
tc(nzero)=zeros(1,length(nzero));

tc_fixed=tc;
tc_fixed(405)=tc(407);
tc_fixed(486:508)=0.1685;
tc_fixed(990:997)=tc(989);
tc_fixed(1345:1417)=tc(1341);
tc_fixed(1741:1749)=tc(1738);   %tc with spikes removed

tc_fixed_smo=smo(tc_fixed,20);  %tc_fixed with smoothing function

gt37q=QSOLVE(tim,tc_fixed_smo,8700,410,25,1,2);
gt37q_smo=smo(gt37q,60);

q1=qtheo(7,750,288,mean(stg(750:1500)),0.035)*ones(length(tim));
```

```
figure(1) plot(tim,stg) xlabel
('Time, t (s)')
ylabel('Stagnation
Pressure, P02 (Pa)')

figure(2)
plot(tim,tc_fixed_smo),
xlabel('Time, t (s)'),
ylabel('Temperature, dT (K)')

figure(3)
plot(tim,gt37q_smo,'b-'),
xlabel('Time, t (s)'),
ylabel('Heat Flux, q"(W/m^2)')

figure(4)
plot(tim(750:1500),q1(750:1500),'k--',tim(750:1500),gt37q_smo(750:1500),'b-'),
hold
plot(tim(750:1500),mean(gt37q_smo(750:1500))*ones(751),'r--')
axis([0.01 0.025 0 110000])
xlabel('Time, t (s)'),
ylabel('HeatFlux,q" (W/m^2)')
legend('Theoretical','Experimental','Experimental mean',4)
```

C.3 Smoothing Function (smo.m)

Script by David Buttsworth

```
function new=smo(old,N);
%
% new=smo(old,N);
% Moving average filter.  At each point in the
% series, the data is smoothed over N points
% forwards and backwards of the that point.
%
% David Buttsworth
% October 2002

len=length(old); new=old; for i=1:N,
   new(1:len-i)=new(1:len-i)+old(1+i:len);
   new(i+1:len)=new(i+1:len)+old(1:len-i);
end; new=new/(2*N+1);
```

C.4 Conduction Heat Transfer (QSOLVE.m)

Script by David Buttworth

```
function Q=qsolve(t,T,rho,c,k,R,cyl)
%

%
% This function returns a heat flux history (as a single column)
% from a given temperature vector for the case when curvature effects
% are significant.  t and q are both column vectors.  Use S.I. units.
%
% The analysis is based on the approximation that the heat conduction
% term (cyl/r).(dT/dr) = (cyl/R).(dT/dr), where R is the radius of
% curvature at the surface and cyl = 0 for a flat plate, 1 for a
% cylinder, and 2 for a sphere.
%
% Thin film properties for calorimeter corrections
%
%rho1=21500;
%c1=130;
%thick=0e-6;
%
% Find the length of the file and the time between data points.
%
numelem=length(t);
deltat=t(2)-t(1);
n=[1:numelem]';
%
sqrtRCK=sqrt(rho*c*k);
alpha=k/rho/c;
const1=2*sqrtRCK/deltat^0.5/pi^0.5;
const2=k*cyl/2/R;
%
% Calculate the flat plate result using the Oldfield, Jones and
% Schultz (1978) formulation (their Eq. 12).
%
Tm(1)=T(1); Tm(2:numelem)=T(1:numelem-1);
Tp(1:numelem-1)=T(2:numelem); Tp(numelem)=T(numelem);
Tnormal(1:numelem)=T;
TT=Tm+Tp-2*Tnormal;
%
Qfp=const1*conv(TT,(n-1).^0.5);
Qfp=Qfp(1:numelem);
%
% Now, the curvature correction term is easy.
%
Tinit=T(1);
```

```
Qcyl=-const2*(T-Tinit);
%
% Now, calculate the calorimeter term.
%
deltaT=0.5*(Tp-Tm);
Qcal=rho1*c1*thick*deltaT/deltat;
%
Q=Qfp+Qcal'+Qcal';
```

C.5 Cook-Felderman Method (qsolve1.m)

```
function qi=qsolve1(t,T,rho,c,k)
%
%This function returns heat transfer vector of length=length(t)-1.
%function is based on Cook-Felderman method,
%where:
%   t   =   time history
%   T   =   Temperature history
%   Rho =   Density
%   c   =   Specific heat
%   k   =   Thermal conductivity
%
%   Brody Roache    2004
%%%%%%%%%%%%%%%%%%%%%%%%%%%%%%%%%%%%%%%%%%%%%%%%%%%%%%%%%%%%%%%%%%%%%%%%%%%%
%
beta=sqrt(rho*c*k);
const=2*beta/pi^0.5;
%
Ti=T(2:length(tim));
Th=T(1:length(tim)-1);
ti=t(2:length(tim));
th=t(1:length(tim)-1);
%
for n=1:length(t)-1;
    qi(n)=0;
    for i=1:n;
        q=(Ti(i)-Th(i))./((th(n)-ti(i))^0.5+(th(n)-th(i))^0.5);
        qi(n)=qi(n)+q;
    end

    qi(n)=qi(n)*const;
end
%
qi=qi';
```

C.6 Convection Heat Transfer (qtheo)

```
function q=qtheo(M,T,Tw,P,D)
%
%This function produces convective heat transfer value for a circular
%flat surface during hypersonic flow.
%Where:
%       M=mach number;
%       T=stagnation Temperature (K);
%       Ts=surface Temperature (K);
%       P=Stagnation Pressure (Pa); and
%       D=Diameter (m);
%
%   Brody Roache    2004
%%%%%%%%%%%%%%%%%%%%%%%%%%%%%%%%%%%%%%%%%%%%%%%%%%%%%%%%%%%%%%%%%%%%%%%%%%%%
%
%Assumptions:
cp=1045;
gamma02=1.36;
gammainf=1.36
Ru=8314.5;
MW=28.96;
R=Ru/MW;

%For ease of calculation of flow functions
gamma=gammainf;
gammac=gammainf-1;
gammad=gammainf+1;
gammae=(gammainf+1)/2;
gammaf=(gammainf-1)/2;

M2=M^2;

%Isentropic Flow functions for compressible flow:
P0P=(1+gammaf*M2)^(gamma/gammac)
T0T=1+gammaf*M2;

gamma=gamma02;
gammac=gamma02-1;
gammad=gamma02+1;
gammae=(gamma02+1)/2;
gammaf=(gamma02-1)/2;

%Normal Shock flow functions:
P02P01=(((gammae*M2)/(1+gammaf*M2))^(gamma/gammac))/
                    ((2*gamma*M2/gammad-gammac/gammad)^(1/gammac))
T2T1=(1+gammaf*M2)*(gamma*M2-gammaf)/(gammae^2*M2);
```

```
%%%%%%%%%%%%%%%%%%----Stagnation Conditions----%%%%%%%%%%%%%%%%%%
rho=P/(R*T)                       %ideal gas law
mu=0.000001458*T^1.5/(T+110.4)  %Sutherland correlation
k=0.001993*T^1.5/(T+112)        %Sutherland correlation


%%%%%%%%%%%%----Stagnation conditions after shock----%%%%%%%%%%%%
P02=P*P02P01
%Stagnation temperature does not change across a normal shock
%therefore:
T02=T;
rho02=P02/(R*T02)
mu02=mu
k02=k;

%%%%%%%%%%%%%%%%%%%%%%----Wall conditions----%%%%%%%%%%%%%%%%%%%%%%
Pw=P02;
rhow=Pw/(R*Tw)
muw=0.000001458*Tw^1.5/(Tw+110.4)  %Sutherland correlation
kw=0.001993*Tw^1.5/(Tw+112)        %Sutherland correlation


%%%%%%%%%%%%%%%%%%----Free Stream Conditions----%%%%%%%%%%%%%%%%%%
Tinf=T/T0T
Pinf=P/(P0P)
rhoinf=Pinf/(R*Tinf)
muinf=0.000001458*Tinf^1.5/(Tinf+110.4)
kinf=0.001993*Tinf^1.5/(Tinf+112)

%Dimensionless numbers
Pr=cp*mu02/k02
Re=rho02*M*(gammainf*R*Tinf)^0.5*D/mu02
KDu=(8*rhoinf/rho02)^0.5;
C=rhow*muw/(rho02*mu02)
%Stagnation point heat transfer for a sphere (White, 1991):
Nu=0.763*Pr^0.4*Re^0.5*C^0.1*KDu^0.5

hc=Nu*kw/D;

%Convection heat transfer equation:
q=hc*(T-Tw);
```

Appendix D

Raw Data

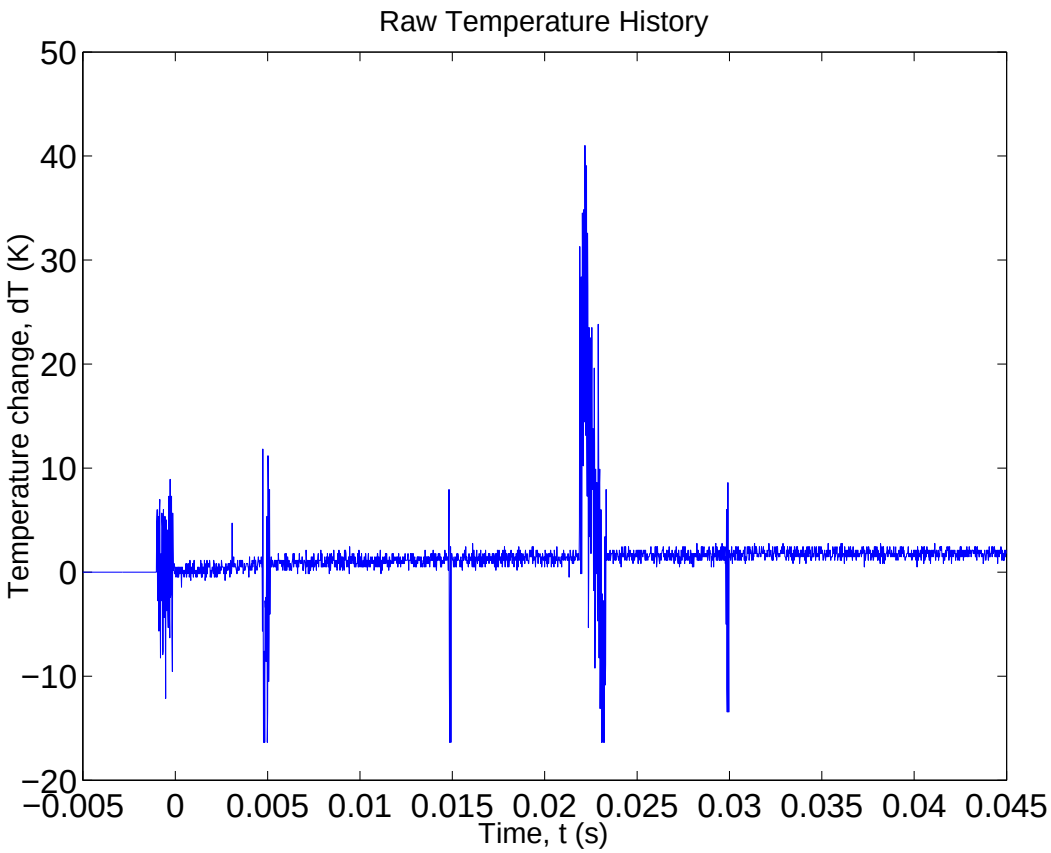
Raw Temperature History
Temperature change, dT (K)
50
40
30
20
10
0
−10
−20
−0.005
0
0.005
0.01
0.015
0.02
0.025
0.03
0.035
0.04
0.045
Time, t (s)

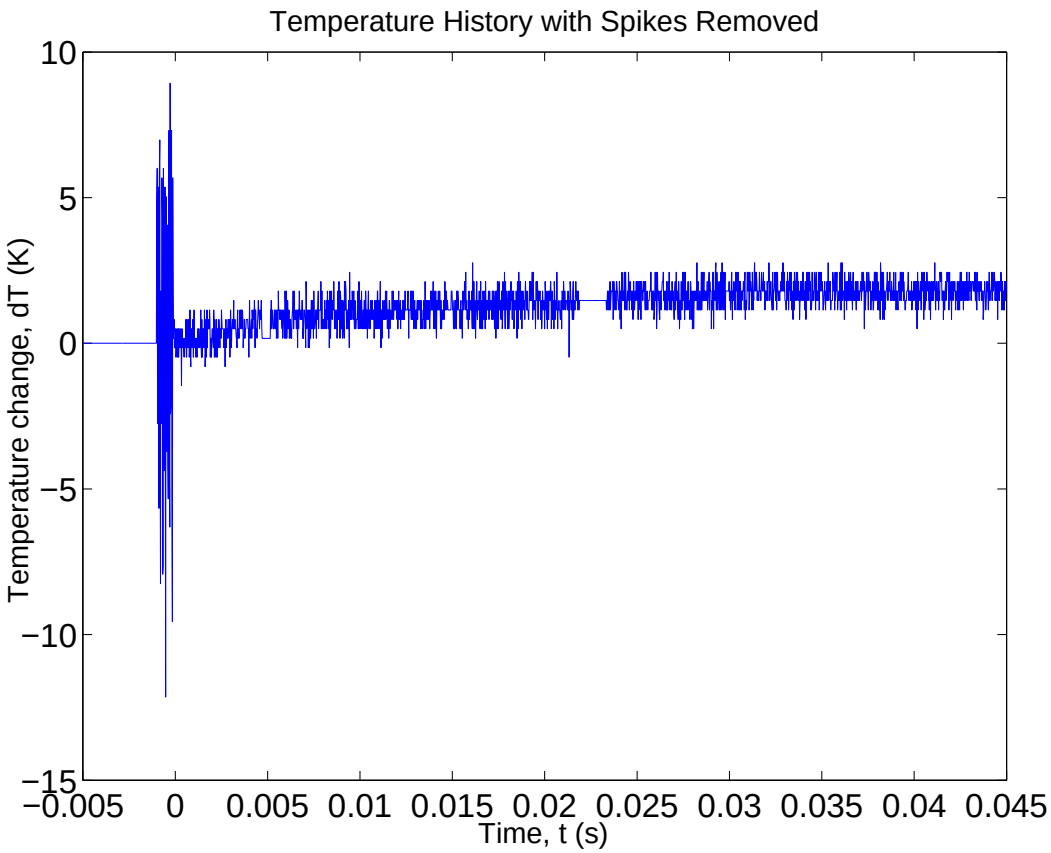
Temperature History with Spikes Removed
Temperature change, dT (K)
Time, t (s)
10
5
0
−5
−10
−15
−0.005
0
0.005
0.01
0.015
0.02
0.025
0.03
0.035
0.04
0.045

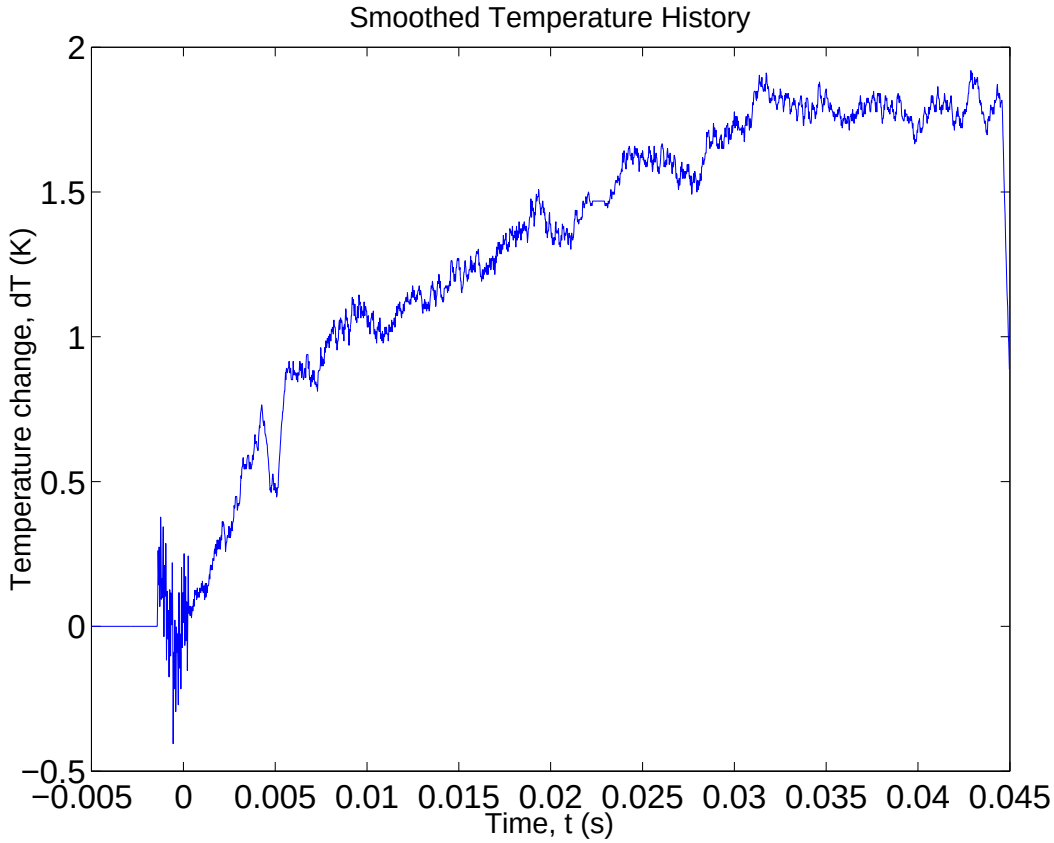
Smoothed Temperature History
Temperature change, dT (K)
Time, t (s)
2
1.5
1
0.5
0
−0.5
−0.005
0
0.005
0.01
0.015
0.02
0.025
0.03
0.035
0.04
0.045

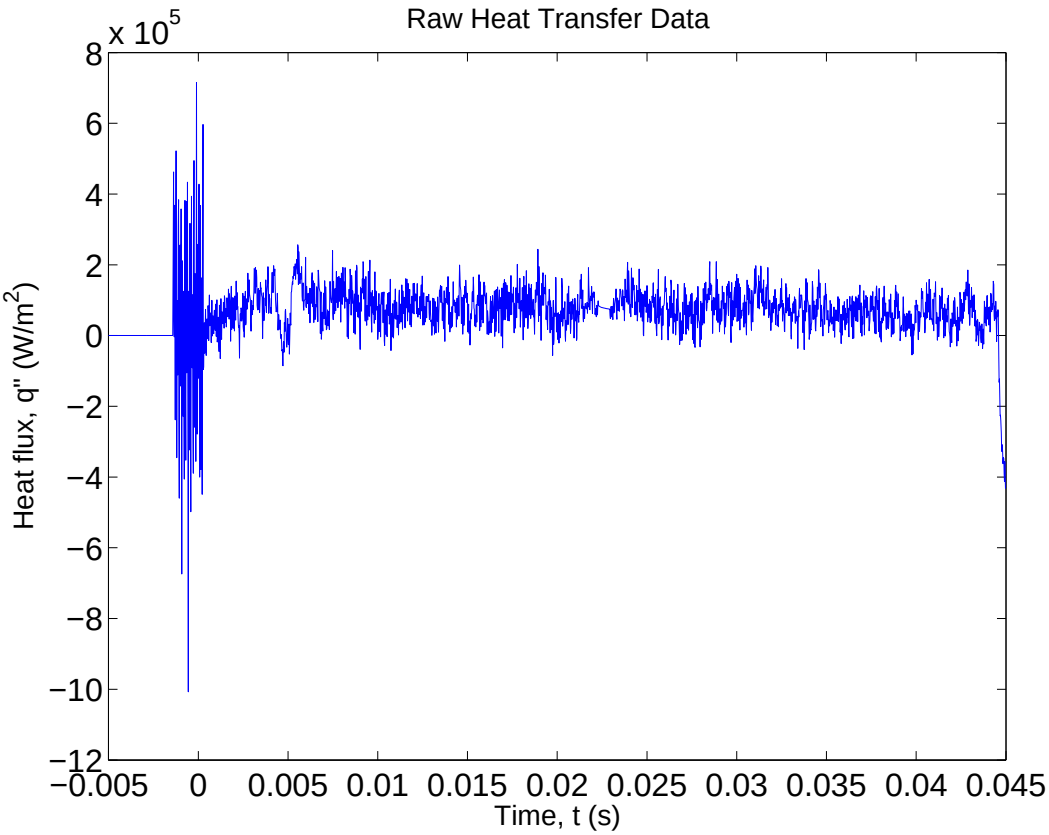
Raw Heat Transfer Data
x 10^5
8
6
4
2
0
−2
−4
−6
−8
−10
−12
Heat flux, q" (W/m^2)
−0.005
0
0.005
0.01
0.015
0.02
0.025
0.03
0.035
0.04
0.045
Time, t (s)

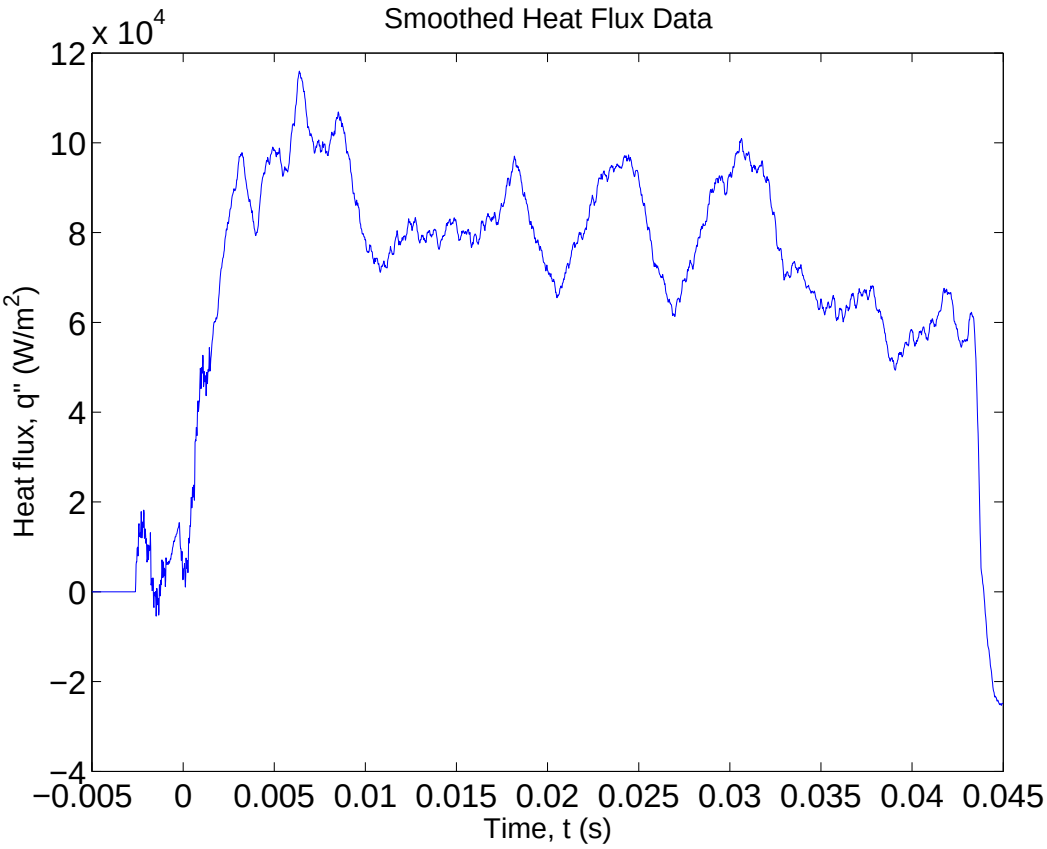
Smoothed Heat Flux Data
x 10^4
12
10
8
6
4
2
0
−2
−4
Heat flux, q" (W/m^2)
−0.005
0
0.005
0.01
0.015
0.02
0.025
0.03
0.035
0.04
0.045
Time, t (s)